Mean-reverting Assets with Mean-reverting Volatility

LO, Yu Wai

A Thesis Submitted in Partial Fulfilment

of the Requirements for the Degree of

Master of Philosophy

in

Risk Management Science

©The Chinese University of Hong Kong

August 2008

Thesis / Assessment Committee

WONG, Hoi Ying (Supervisor)
LEUNG, Pui Lam William (Chairman)
CHAN, Ngai Hang (Committee Member)
WU, Li-xin (External Examiner)

Abstract of thesis entitled:

Mean-Reverting Assets with Mean-Reverting Volatility

Submitted by Lo Yu Wai

for the degree of Master of Philosophy in Risk Management Science

at The Chinese University of Hong Kong in August 2008.

ABSTRACT

Many underlying assets of option contracts, such as currencies, commodities, energy, temperature and even some stocks, exhibit both mean reversion and stochastic volatility. This thesis investigates the valuation of options when the underlying asset follows a mean-reverting lognormal process with two different stochastic volatility models. In the first case, we consider a one factor SV model consistent with the Heston (1993) approach. A closed-form solution is derived for European options by means of Fourier transform. The proposed model allows the option pricing formula to capture both the term structure of futures prices and the market implied volatility smile within a unified framework. A bivariate trinomial lattice approach is introduced to value path-dependent options with the proposed model. Numerical examples using European options, American options and barrier options demonstrate the use of the model and the quality of the numerical scheme.

In the second case, the stochastic volatility is driven by two stochastic processes with one persistent factor and one fast mean-reverting factor. Semi-analystical pricing formulas for European option is derived by means of multiscale asymptotic techniques.

摘要

很多期權合約的相關資產如貨幣、商品、能源、溫度甚至股票均呈現平均數復歸及隨機波幅。本文研究當相關資產價格行為依循平均數復歸的對數常態過程及兩種不同的隨機波幅模型時期權的定價。其中一種研究的隨機波幅模型為Heston模型。歐式選擇權的定價方程式可利用傅利葉轉換從而建立。本文建議模型的期權定價方程式能在統一架構下同時捕捉期子價格及市場所見的波幅微笑。本文亦介紹如何在建議模型下利用雙變三項式的格子方法對取決於軌道的期權定價。利用關於歐式期權，美式期權及定界期權的數值例子,我們展示出本文所建議的模型的作用及所介紹的數值計算法的準確性。

另一種隨機波幅模型為多尺度隨機波幅模型。模型內的隨機波幅由兩組隨機過程控制，一組為持續性的因素，另一組為快速平均數復歸的因素。利用多尺度漸近的技術，我們求出歐式期權的半解析定價方程式。

THE CHINESE UNIVERSITY OF HONG KONG
GRADUATE SCHOOL

The undersigned certify that we have read a thesis, entitled "Option Pricing with Mean Reversion and Stochastic volatility" submitted to the Graduate School by Lo, Yu Wai (羅裕偉) in partial fulfilment of the requirements for the degree of Master of Philosophy in Statistics. We recommend that it be accepted.

_____

Prof. Wong Hoi-ying

Supervisor

_____

Prof. Chan Ngai-hang

_____

Prof. Leung Pui-lam

_____

Prof. Wu Li-xin

External Examiner

DECLARATION

No portion of the work referred to in this thesis has been submitted in support of an application for another degree or qualification of this or any other university or other institution of learning.

ii

ACKNOWLEDGEMENT

Contents

List of Figures

Chapter 1

Introduction

Evidence on mean reversion in financial assets is abundant. In particular, there is a census that commodity prices cannot increase exponentially but rather revert to their equilibrium mean levels. Supportive theoretical arguments and empirical evidence have been produced by Cecchetti et. al. (1990) and Bessembinder et al. (1995), respectively. It has been documented that currency exchange rates also exhibit mean reversion. Jorion and Sweeney (1996) show how the real exchange rates revert to their mean levels and Sweeny (2006) provides empirical evidence of mean reversion in G-10 nominal exchange rates. More interestingly, but not surprisingly, mean reversion also appears in some stock prices as evidenced by Poterba and Summers (1988).

Derivative pricing with mean reversion has been an important topic in financial engineering. Most of the related research has concentrated on the commodity, currency, energy and temperature derivatives markets. A possible reason for the

last market is that standardized futures contracts written on temperature indices have been traded on the Chicago Mercantile Exchange since October 2003, together with European call and put options written on these futures. The temperature indices are based on measurement locations in the US and Europe.

Scientists have had the idea of using mean-reverting models for average temperatures, because their values should revert to deterministic mean levels that are trends due to global warming and obvious seasonality. Doernier and Querel (2000) propose an Ornstein-Uhlenbeck dynamics with a time-dependent volatility but only use constant parameters in their analysis of the Chicago temperature data. Alaton et al. (2002) employ a similar model for data collected from Bromma and Sweden. Benth and Saltyte-Benth (2007) propose a mean reverting process with a seasonal volatility to fit temperature data and derive the corresponding explicit pricing formulas for temperature futures and options.

In currency option pricing, Sorensen (1997) advocates mean reversion through the dynamics in the domestic and foreign term structures of interest rates. Ekvall et al. (1997) give several reasons for mean-reverting exchange rates using an equilibrium model and derive the closed-form solution of European options. One possible reason for mean reversion in the foreign-exchange market is the intervention of central banks that keeps the exchange rates close to desired target values. Thus, the mean-reversion speed can be regarded as a measure for the magnitude of the central bank intervention. The approach of Ekvall et al. (1997) has been applied to path-dependent currency option pricing by Hui and Lo (2006), and

2

Wong and Lau (2008).

Another important feature of financial assets is their stochastic volatility. A typical SV model assumes that volatility is driven by a mean-reverting process. Hull and White (1987) examined the pricing of vanilla options with this model. Heston (1993) proposed a squared-root mean-reverting process for the volatility, and obtained analytical formulas for options on bonds and currency in terms of characteristic functions. Using tick-to-tick data of S&P 500, Fouque et al. (2000) observed a fast timescale volatility factor that the mean-reverting rate reached the order of 200. They then derived a perturbation solution for European options in a fast mean-reverting SV economy. Their model has been applied to value exotic options [for an example see Cotton et al.(2004), Wong and Cheung (2004), and Ilhan et al. (2004)].

Empirical tests, however, suggest that one factor SV models are inadequate to either describe the evolution of financial time series or capture the volatility smile. The empirical results of Fiorentini et al. (2002) indicate that the Heston model has a tendency to overprice out-of-the money (underprice in-the-money) calls for daily data. Daniel et al. (2005) constructed a goodness-of-fit test for the Heston model and showed that it fails to provide a statistically acceptable fit to data. Andersen and Bollerslev (1997) examined the intraday periodicity and the volatility in foreign exchange and equity markets, and found that several distinct component processes affected the volatility dynamics. In other words, there should be more than one factor in the SV process. When the spectral

3

generalized method of moments was applied to one-factor SV models, Chacko and Viccira (2003) observed that the estimate of the mean-reverting rate increased dramatically with the sampling frequency of the observed data. They proposed that the volatility was a sum of several mean-reverting processes that shared the same long term mean and volatility, but differed in the mean-reverting rate. The empirical study of Alizadeh et al. (2002) documented that there were two dominated stochastic factors that governed the evolution of volatility, with one highly persistent factor and one quickly mean-reverting factor. Chernov et al. (2003) also found evidence in favor of a second volatility factor. In fact, LeBaron (2001) has documented that two-factor SV models can produce the kurtosis, fat-tailed return distribution and long memory effect that is observable in many financial time series.

Recently, multi-factor SV (MSV) models have generated attention from the option pricing literature. Duffie et al. (2000) analyzed option pricing for affine jump diffusions which include multi-factor affine volatility models as a special case. Van der Ploeg et al. (2003) attempted to estimate the multi-factor affine SV option pricing models with a state space approach. Fouque et al. (2003b) proposed a multiscale volatility model that was based on the suggestion of Alizadeh et al. (2002) and others, and managed to calibrate all effective parameters from volatility smiles. They also obtained an analytic approximation of a European call option as the sum of the BS formula and the Greek correction term. The Greek correction term is a combination of the gamma, delta-gamma, vega, and

delta-vega of the option.

This thesis combines the aforementioned indispensable features of financial assets and investigates the valuation of options when the underlying asset follows a mean-reverting lognormal process with two different stochastic volatility models. In the first case, we consider a one factor SV model consistent with the Heston (1993) approach and develop a unified option pricing framework. The proposed model enables option prices to be simultaneously consistent with observed future prices and the volatility smile of the option market. Closed-form solutions for vanilla call and put options are derived by means of Fourier transform. A numerical method based on a bivariate trinomial lattice approach is constructed to value path-dependent options, such as barrier and American options, using the proposed model. Numerical examples show that our model can generate realistic volatility smile and the numerical method offers an efficient computation for exotic option prices.

The proposed model is flexible enough for a financial analyst to perform scenario analysis with it. For instance, a currency option trader who is concerned about the impact of central bank intervention on option prices can examine the sensitivity of the option price to the change in mean-reversion speed. To allow seasonal volatility in temperature derivative pricing, the mean level of the volatility process can be postulated to be a time-dependent periodic function. In such a situation, the closed-form solutions for vanilla call and put options are still available.

A study closely related to this is that by Deng (1999), who presents a general road map for energy derivative pricing with mean reversion, jumps and spikes. As his model is very general, no closed-form solution can be obtained, even for vanilla options and the characteristics function, and all of the calculations should resort to numerical methods on integral differential equations. This thesis introduce the mean-reverting underlying process with the Heston (1993) volatility model so that closed-form solutions for vanilla options become possible. This greatly reduces the computational time for calibrating model parameters, retains analytical tractability and captures the two important features of financial assets at once. Moreover, the proposed trinomial lattice approach adds negligible computational burden compared to the existing two-dimensional trinomial lattice approaches.

In the second case, the evolution of stochastic volatility is driven by the aforementioned two dominated stochastic factors, with one highly persistent factor and one quickly mean-reverting factor. Semi-analystical pricing formulas for European option is derived by means of multiscale asymptotic techniques. This thesis contributes the literature in that asymptotic approximation and its accuracy to prices of European options under the two-factor SV model and mean-reverting lognormal underlying process is derived and shown.

The rest of this thesis is organized as follows. Chapter 2 reviews the mean reverting model, volatility smile and SV models. A brief introduction on the multiscale stochastic volatility model of Fouque et al. (2003b) is also given.

6

Chapter 3 presents the proposed mean reversion model with the Heston stochastic volatility, examines the corresponding distributional properties, and derives the characteristic function of the log-asset value. Speciafically, a closed-form solution is derived for general European options by means of Fourier transform. The effect of the proposed model to the implied volatility smile is reported. We also establish the two-dimensional trinomial lattice approach to valuing options with path-dependent features. Chapter 4 gives details of the multiscale SV model for a mean-reverting underlying asset. Specifically, the partial differential equation (PDE) is obtained for a European option. An asymptotic solution to the PDE is then established by means of singular perturbation technique of Fouque *et al.* (2003b). The accuracy of the analytic approximation is also investigated. Chapter 5 concludes the thesis.

Chapter 2

Literature Review

In this chapter, we introduce the mean-reverting model, volatility smile and stochastic volatility (SV) models.

2.1 Mean-reverting Model

Mean reversion is a tendency for a stochastic process to remain near, or return over time to a long-run average. An example of mean reversion is illustrated in Figure 2.1. Mean-reverting models have long been used for modeling financial assets. For example, interest rate appears to be pulled back to some long-run average level over time. When interest rate is high, mean reversion tends to cause it to have a negative drift; when interest rate is low, mean reversion tends to cause it to have a positive drift. There are compelling economic arguments in favour of mean reversion. When rates are high, the economy tends to slow down and there is low demand for funds from borrowers. As a result, rates decline.
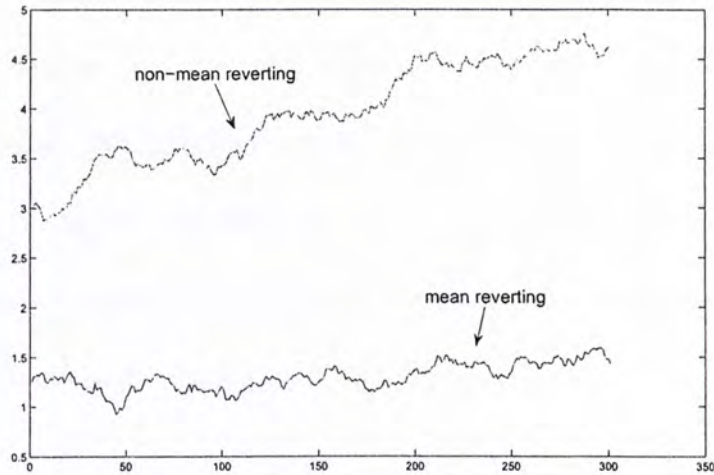
Figure 2.1: example on mean reversion

When rates are low, there tends to be a high demand for funds on the part of borrowers and rate tends to rise.

Hull and White (1990) explored extensions of the Vasicek Model that provide an exact fit to the initial term structure. One version of the extended Vasicek model that they consider is

$$dr_t = a(\frac{\theta(t)}{a} - r_t)dt + \sigma dW_t,$$

where r_t is the short rate at time t, W_t is the Wiener process, a and σ are constants. This is know as the Hull-White Model. It can be characterized as the Vasicek model with a time-dependent reversion level.

Scientists have also had the idea of using mean-reverting models for average temperatures, because their values should revert to deterministic mean levels that are trends due to global warming and obvious seasonality. Doernier and Querel

9

(2000) propose an Ornstein-Uhlenbeck dynamics with a time-dependent volatility but only use constant parameters in their analysis of the Chicago temperature data. Alaton et al. (2002) employ a similar model for data collected from Bromma and Sweden. Benth and Saltyte-Benth (2007) propose a mean-reverting process with a seasonal volatility to fit temperature data. The mean-reverting model proposed by Benth and Saltyte-Benth (2007) is as follows:

$$dT(t) = ds(t) - \kappa(T(t) - s(t))dt + \sigma(t)dW(t),$$

where κ is the mean-reverting speed, $W(t)$ is the Wiener process, $s(t)$ is a deterministic function modeling the trend and seasonality of temperature and $\sigma(t)$ describes the daily volatility of temperature variations. $s(t)$ and $\sigma^2(t)$ are of the form

$$s(t) = a + bt + a_0 + \sum_{i=1}^{I_1} a_i sin(2i\pi(t - f_i)/365) + \sum_{j=1}^{J_1} b_j cos(2j\pi(t - g_j)/365),$$

and

$$\sigma^2(t) = c + \sum_{i=1}^{I_2} c_i sin(2i\pi t/365) + \sum_{j=1}^{J_2} d_j cos(2j\pi t/365).$$

Using the aforementioned model, Benth and Saltyte-Benth (2007) derive the corresponding explicit pricing formulas for temperature futures and options.

In currency option pricing, one possible reason for mean reversion in the foreign-exchange market is the intervention of central banks that keeps the exchange rates close to desired target values. Thus, the mean-reversion speed can be regarded as a measure for the magnitude of the central bank intervention.

Sorensen (1997) advocates mean reversion through the dynamics in the domestic and foreign term structures of interest rates. Ekvall et al. (1997) give several reasons for mean-reverting exchange rates using an equilibrium model and derive the closed-form solution of European options. The approach of Ekvall et al. (1997) has been applied to path-dependent currency option pricing by Hui and Lo (2006), and Wong and Lau (2008) with the model shown as follows:

$$\frac{dF_t}{F_t} = [\kappa(\log \bar{F} - \log F_t) + (r - r_f)]dt + \sigma dW_t,$$

where $\bar{F}$ is the conditional mean exchange rate, κ is the speed of reversion, σ is the volatility of the exchange rate, r is the domestic interest rate, r_f is the foreign interest rate, and W_t is the Wiener process.

2.2   Volatility Smile

Black and Scholes (1973) assume the following asset price dynamics:

$$\frac{dS_t}{S_t} = (\mu - q)dt + \sigma dW_t,$$

where S_t is the asset price at time t, W_t is the Wiener process, μ, q and σ are constant parameters representing drift, dividend yield and volatility respectively. For a call option with payoff $\max(S_T - K, 0)$, Black and Scholes derive the pricing formula:

$$\begin{aligned}
V_{BS}(t, S_t) &= S_t e^{-q(T-t)} N(d^+) - K e^{-r(T-t)} N(d^-), &(2.1)\\
\text{where} \qquad d^{\pm} &= \frac{\ln(S_t/K) + (r - q \pm \sigma^2/2)(T-t)}{\sigma\sqrt{T-t}},
\end{aligned}$$

where t is the current time, K is the strike price of the option, T is the maturity of the option and r is the risk free interest rate.

In (2.1), the only parameter that is not directly observable is the volatility, σ. Market practitioners usually estimate it by calibrating to traded options data. That means they set market price to be equal to the BS price and then extract the volatility. The volatility obtained in this way is called the implied volatility. This method worked quite well in the early 1980s. However, after the stock market crashed in Black Monday on 19 October 1987, there is an effect called volatility skew/smile observed in the derivatives market.

After the market crashed, it is discovered that the implied volatility decreases with the moneyness , the strike price over the current asset price (K/S). The skew effect is not compatible with the model assumption that the volatility is a constant.

Rubinstein (1994) suggests that the reason for this effect may be of "crashophobia", the awareness of stock crash like the Black Monday. This results in the market practitioners believe that returns should not follow a normal distribution, rather a distribution that has heavier tails. Therefore two classes of models are proposed to capture the skew effect. They are jump-diffusion models and SV models. In this thesis, we focus on the SV models.

2.3 Stochastic Volatility Model

Stochastic volatility model is similar to the Black-Scholes model, except that the volatility is driven by stochastic variable(s). In 1987, Hull and White (1987) introduce the asset price dynamics with a stochastic volatility. They model the instantaneous variance as a Geometric Brownian Motion that is independent to the asset return and derive the analytical solution for European options. Stein and Stein (1991) view the volatility itself as a mean-reverting process. Mean reverting process is a process that is pulled backed to the long-run average over time. They obtained an analytical solution by assuming the volatility process to be uncorrelated with the asset dynamics.

Heston (1993) relaxed the assumption of Stein and Stein (1991) to allow correlation between assets and volatility. Then, closed form solutions are derived for bond and currency options in terms of characteristic functions. Computation can be implement by using numerical Fourier inversion.

Fouque *et al.* (2000) examine the S & P 500 option data and discover that one factor governing the volatility follows a fast mean-reverting process. It means that the mean-reverting rate is high. They model the volatility as a positive function with a latent factor, which follows a fast-mean reverting process. They perform perturbation techniques to obtain European and American option prices. Under this framework, a large number of parameters can be reduced into two grouped parameters only. Moreover, the perturbation solution solely depends on these two

grouped parameters, the Black-Scholes price and Greeks. The most attractive thing of this approach is that the two grouped parameters can be calibrated with a simple linear regression.

Unfortunately their approach has its weakness. Since the skewness of the volatility smiles varies across maturities, a simple linear regression may not be able to capture the whole volatility surface. Under their approach, the implied volatility surface implied by European options is given by

$$\sigma_I \simeq \overline{\sigma} + b^\epsilon + a^\epsilon \frac{\ln(K/S)}{T-t},$$

where σ_I is the implied volatility and the parameters ($\overline{\sigma}$, a^ϵ, b^ϵ) are used to obtain the two grouped parameters. $\overline{\sigma}$ is estimated from historical daily index value over one month horizon. After regressing σ_I on log-moneyness to maturity ratio (LMMR), we can calibrate a^ϵ and b^ϵ. Also, LMMR is defined as $\frac{\ln(K/S)}{T-t}$.

Although the approach of Fouque et al. (2000) is inadequate to capture volatility surface, many researches appeared to price exotic products under this framework. For instance, pricing formulas on Asian options, barrier options, lookback options and interest rate derivatives are derived in Fouque and Han (2003), Cotton et al. (2004), Wong and Cheung (2004) and Ilhan et al. (2004).

Empirical studies also suggest that stochastic volatility should consist of two factors, a slow timescale factor and a fast timescale factor. Alizeth et al. (2002) perform an empirical study on stochastic volatility model to show the mentioned result empirically. This motivates people to explore the effect of multiscale SV

on derivatives pricing.

2.4 Multiscale Stochastic Volatility Model

Fouque *et al.* (2004) develop a framework to price European options under the multiscale SV environment. Similarly, the advantage of their approach is that grouped parameters can be calibrated easily. They model the volatility as a positive function of two latent variables, one follows a fast mean-reverting process and the other one follows a slow mean-reverting process. They derive analytical formulas for European option prices by using perturbation technique. The solution is expressed in terms of four grouped parameters, the Black-Scholes price and Greeks. The four grouped parameters can be calibrated through multiple linear regression.

The approach of Fouque *et al.* (2004) outperforms that of Fouque *et al.* (2000) on capturing volatility surface. Under their approach, the volatility surface implied by European option data is given by

$$\sigma_I \simeq \overline{\sigma}(z) + \left[b^\epsilon + b^\delta(T - t)\right] + \left[a^\epsilon + a^\delta(T - t)\right]\frac{\ln(K/S)}{T - t},$$

where the parameters $(\overline{\sigma}(z), a^\epsilon, b^\epsilon, a^\delta, b^\delta)$ are related to the four effective grouped parameters. $\overline{\sigma}(z)$ is estimated from historical daily index value over one month horizon. After regressing σ_I on time to maturity, log-moneyness and the interaction term, LMMR, we obtain a^ϵ, b^ϵ, a^δ and b^δ. This approach has been applied to Lookback options, dynamic fund protection and turbo warrants by Wong and

Chan (2007, 2008).

In this thesis, we not only discuss Heston type stochastic volatility model with mean-reverting asset dynamic but also investigate the impact of multiscale SV by using Fouque *et al.* (2004) approach.

Chapter 3

The Heston Stochastic Volatility

In this chapter, we introduces the proposed mean reversion model with stochastic volatility following heston model. The corresponding distributional properties is examined and the characteristic function of the log-asset value is also derived. A closed-form solution is derived for general European options by means of Fourier transform. The effect of the proposed model to the implied volatility smile is reported. We also establishes the two-dimensional trinomial lattice approach to valuing options with path-dependent features.

3.1 The Model

The proposed model assumes that the underlying asset, S_t, has the following dynamics, under risk-neutral measure,

$$S_t = \exp(X_t),$$

$$dX_t = \left[\theta(t) - \kappa X_t - \frac{v_t}{2}\right]dt + \sqrt{v_t}dW_t^{(0)}, \qquad (3.1)$$

$$dv_t = (a(t) - bv_t)dt + \sigma\sqrt{v_t}dW_t^{(1)},$$

where the constant κ is the mean-reversion speed for the asset; the constant b is the mean-reversion speed of the volatility; the deterministic function $\theta(t)$ represents the equilibrium mean level of the asset against time; the function $a(t)$ is the equilibrium mean level of the volatility against time; the process v_t is the volatility of the underlying asset, which follows the Heston (1993) stochastic volatility model; the constant σ is the volatility coefficient of the volatility process; and $W_t^{(0)}$ and $W_t^{(1)}$ are correlated Wiener processes with correlation coefficient ρ. This proposed model is reduced to the Heston model if the mean-reversion speed, κ, is equal to zero.

3.1.1 The Characteristic Function

Given the dynamic of the underlying asset, it is possible to obtain the characteristic function for the log-asset value X_t. Denote the characteristic function as

$$f(x, v, t; \phi) = E[e^{i\phi X_T}|X_t = x, v(t) = v], \qquad (3.2)$$

where $T \geq t$ and $i = \sqrt{-1}$. Then, the following lemma holds.

Lemma 3.1.1. Suppose that X_t follows the dynamics in (3.1). Then, the characteristic function for X_T defined in (3.2) is given by

$$f(x, v, t; \phi) = \exp\left[B(T - t) + C(T - t)x + D(T - t)v + i\phi x\right],$$

18

where

$$B(\tau) = i\phi \int_{T-\tau}^{T} \theta(s)e^{-\kappa(T-s)}ds + \int_{T-\tau}^{T} a(s)D(T-s)ds,$$

$$C(\tau) = i\phi e^{-\kappa\tau} - i\phi,$$

$$D(\tau) = U(e^{-\kappa\tau}) + \frac{e^{-b\tau}V(e^{-\kappa\tau})}{-\frac{1}{U(1)} + \frac{\sigma^2}{2k}\int_{1}^{e^{-\kappa\tau}} y^{\frac{b}{\kappa}-1}V(y)dy},$$

$$U(y) = \frac{2\kappa y}{\sigma^2} \frac{(\sqrt{1-\rho^2}-\rho i)\frac{\sigma\phi}{2\kappa}\Phi(a^*,b^*,\frac{y}{\lambda}) + \frac{a^*}{b^*\lambda}\Phi(a^*+1,b^*+1,\frac{y}{\lambda})}{\Phi(a^*,b^*,\frac{y}{\lambda})},$$

$$V(y) = \frac{\Phi^2(a^*,b^*,\frac{1}{\lambda})}{\Phi^2(a^*,b^*,\frac{y}{\lambda})}e^{\frac{\sigma\phi}{\kappa}(1-y)\sqrt{1-\rho^2}},$$

$$a^* = \frac{(\sqrt{\rho^2-1}+\rho)\frac{b^*}{2} + \frac{\sigma}{4\kappa}}{\sqrt{\rho^2-1}},$$

$$b^* = 1 - \frac{b}{\kappa}, \quad \lambda = \frac{-\kappa}{\sigma\phi\sqrt{1-\rho^2}}, \quad \tau = T - t,$$

and $\Phi(\cdot,\cdot,\cdot)$ is the degenerated hypergeometric function.

Proof. See Appendix , where basic properties of the degenerated hypergeometric function are also introduced. $\square$

The degenerated hypergeometric functions are also known as the confluent hypergeometric functions or Whittaker functions available in the Mathematica and Matlab software packages. These mathematical functions are widely applied in mathematics, physics and engineering. In finance, these appear in, but are not limited to, Davydov and Linetsky (2001), Cadenillas et al. (2007), Wong and Chan (2008), and Wong and Lau (2008).

The probability density function of the log-return can be obtained through inverting the Fourier transform on the characteristic function. Here, we examine the distributional properties of the proposed model. Figure 3.1 shows how a
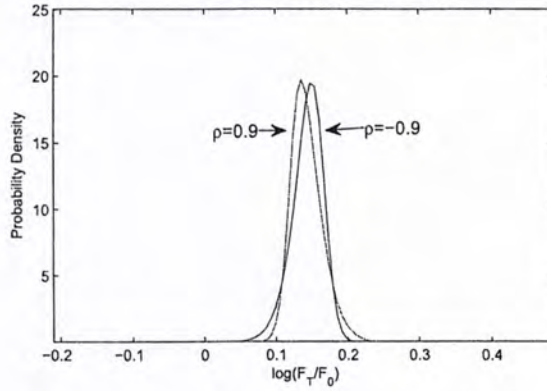
Figure 3.1: Probability density function of the log-return over a 1-year horizon with different correlations. Parameter values are: $\kappa = 10, \theta(t) \equiv 4.0647, b = 2, a(t) \equiv 0.01b, \sigma = 0.1, v_0 = 0.01, S_0 = 1.3$.

positive correlation of volatility with the spot return creates a fat right tail and a thin left tail distribution of the log-return. As a positive correlation results in high variance when the spot asset rises, and this fattens the right tail of the density function. That effect is consistent with the Heston (1993) model, which only considers geometric Brownian motion for the underlying asset.

Figure 3.2 shows how the mean-reversion rate of the underlying asset pushes the distribution more towards the equilibrium mean level $\theta(t)$. If we interpret the underlying asset as an exchange rate, then the mean-reversion rate can be regarded as an indicator of the magnitude of central bank intervention, which drives the exchange rate back to the level specified by the central bank. Thus, an increase in the magnitude of central bank intervention on the exchange rate results in a decrease of the variance of the log-return.
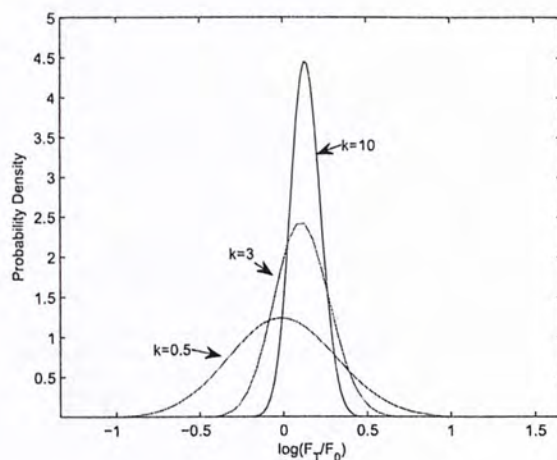
Figure 3.2: Probability density function for different values of κ. Parameter values are: $\theta(t) \equiv \kappa \ln(1.5), b = 3.33, a(t) \equiv 0.16b, \sigma = 0.04, v_0 = 0.18, \rho = 0.9, S_0 = 1.3$.

Figure 3.3 shows how the mean-reversion rate of the volatility process affects the log-return distribution. As the equilibrium variance level is lower than current variance in our example, a large value of b quickly pushes the variance to the equilibrium variance level and hence makes both tails thin. However, if the equilibrium variance level is higher than the realized variance, then the distribution should have a fatter tail.

As pointed out by Heston (1993) and many others, the characteristic function is not only useful for examining distributional properties but also for deriving formulas for standard derivative products. An obvious application is to derive a closed-form solution for forward (future) prices.

Under the risk-netrual dynamics (3.1), a forward price of the underlying asset

21
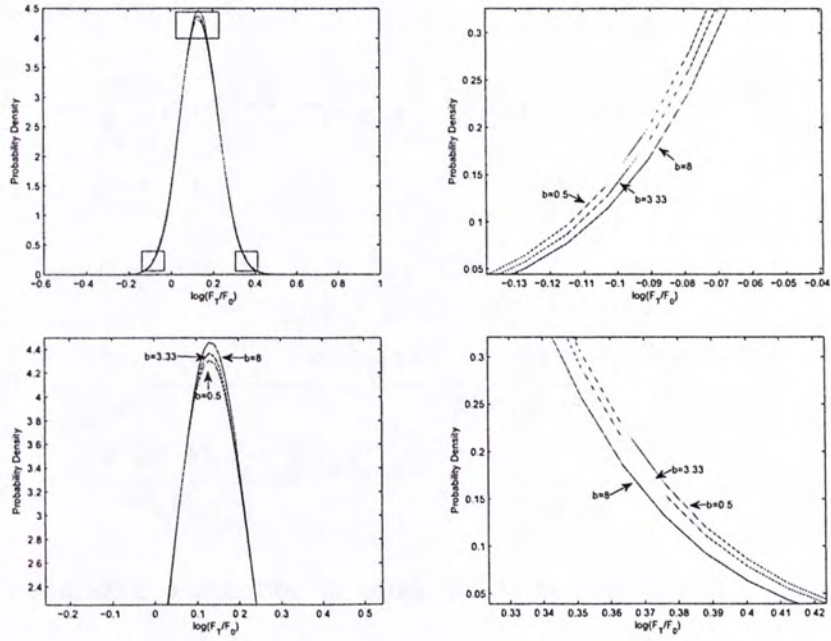
Figure 3.3: Probability density function for different values of b. Parameter values are: $\theta(t) \equiv 4.0647, \kappa = 10, a(t) \equiv 0.16b, \sigma = 0.04, v_0 = 0.18, \rho = 0.9, S_0 = 1.3$.

S_t with maturity T is given by

$$F_T(t) = E_t(S_T) = f(x, v, t; -i),$$

where $f(x, v, t; \phi)$ is defined in (3.2). Lemma 3.1.1 immediately gives the following.

Corollary 3.1.1. The forward price of an asset following MRSV (3.1) is given by,

$$F_T(t) = \exp\left[B_F(\tau) + C_F(\tau)x + D_F(\tau)v + x\right],$$

22

where $x = \ln S, \tau = T - t,$

$$B_F(\tau) = \int_{T-\tau}^{T} \theta(s) e^{-\kappa(T-s)} ds + \int_{T-\tau}^{T} a(s) D_F(T-s) ds,$$

$$C_F(\tau) = e^{-\kappa\tau} - 1,$$

$$D_F(\tau) = U_F(e^{-\kappa\tau}) + \frac{e^{-b\tau} V_F(e^{-\kappa\tau})}{-\frac{1}{U_F(1)} + \frac{\sigma^2}{2\kappa} \int_1^{e^{-\kappa\tau}} y^{\frac{b}{\kappa}-1} V_F(y) dy},$$

$$U_F(y) = \frac{2\kappa y}{\sigma^2} \frac{-(\sqrt{\rho^2 - 1} + \rho) \frac{\sigma}{2\kappa} \Phi(a^*, b^*, \frac{y}{\lambda_F}) + \frac{a^*}{b^* \lambda_F} \Phi(a^* + 1, b^* + 1, \frac{y}{\lambda_F})}{\Phi(a^*, b^*, \frac{y}{\lambda_F})},$$

$$V_F(y) = \frac{\Phi^2(a^*, b^*, \frac{1}{\lambda_F})}{(a^*, b^*, \frac{y}{\lambda_F})} e^{\frac{\sigma}{\kappa}(y-1)\sqrt{\rho^2-1}}, \quad \lambda_F = \frac{\kappa}{\sigma\sqrt{\rho^2 - 1}}.$$

Let us imagine a situation in which the term structure of forward (future) prices is observed at time t. In practice, it is often useful to express the characteristic function in terms of the observed term structure of forward prices. More precisely, we would like to calibrate the characteristic function to observed forward prices. This is important for deriving option pricing formulas that are consistent with the observed forward prices in the next section.

We now carry out the super-calibration by directly expressing the characteristic function in terms of observed market forward (future) prices. There is a common term in $B(\tau)$ of Lemma 3.1.1 and $B_F(\tau)$ of Corollary 3.1.1, which is

$$\int_t^T \theta(s) e^{-k(T-s)} ds = \ln(F_T(t)) - C_F(\tau)x - D_F(\tau)v - x - \int_t^T a(s) D_F(T-s) ds.$$

Substituting it into Lemma 3.1.1, we obtain the following proposition.

Proposition 3.1.1. If the underlying asset follows the MRSV process (3.1), then the characteristic function calibrated to the term structure of future prices is given

23

by

$$f(x, v, t; \phi, F_T(t)) = F_T(t)^{i\phi} \exp\left[\Delta B(t, T) + \Delta D(t, T)v\right],$$

where

$$\Delta B(t, T) = \int_t^T a(s)\Delta D(s, T)ds,$$
$$\Delta D(t, T) = D(\tau) - i\phi D_F(\tau),$$

with $\tau = T - t$, $D(\tau)$ defined in Lemma 3.1.1, and $D_F(\tau)$ defined in Corollary 3.1.1.

3.2   European Option Pricing

Once the characteristic function is found, European options can be valued using Fourier inversion. Carr and Madan (1999) advocate the Fast Fourier Transform (FFT) to compute vanilla call and put options based on the characteristic function of the log-asset value. Lewis (2001) presents a method to compute European options with arbitrary payoff functions. This section demonstrates how these methods can be applied to our case, and it also examines the shape of the Black-Scholes implied volatilities given by the proposed model. We attempt to show numerically that the proposed model not only fits the term structure of future prices but also generates a realistic volatility smile consistent with the market.

24

3.2.1 Plain Vanilla Options

The plain vanilla call option has the payoff:

$$\max(S_T - K, 0),$$

where K is the strike price and T is the option's maturity. Let k denote the log of the strike price K, $C_T(k)$ be the desired value of a T-maturity call option with strike $\exp(k)$, and $q_T(s)$ be the risk-neutral density of the log-asset price $s_T = \ln S_T$.

Following Carr and Madan (1999), the modified call price $c_T(k)$ is defined by:

$$c_T(k) = \exp(\alpha k)C_T(k), \quad \text{for some constant } \alpha > 0,$$

where $C_T(k) = \int_k^\infty e^{-rT}(e^s - e^k)q_T(s)ds$. As $C_T(k)$ is not square integrable over $(-\infty, \infty)$, the introduction of a damping factor $\exp(\alpha k)$ aims at removing this problem. This makes the Fourier transform of $c_T(k)$ exist:

$$\psi_T(\xi) = \int_{-\infty}^{\infty} e^{i\xi k}c_T(k)dk = \frac{e^{-rT}f(x, v, t; \phi = \xi - (\alpha + 1)i)}{\alpha^2 + \alpha - \xi^2 + i(2\alpha + 1)\xi}, \quad (3.3)$$

where f is the characteristic function defined in Proposition 3.1.1.

Call prices can then be numerically obtained by using the inverse transform:

$$C_T(k) = \frac{e^{-\alpha k}}{2\pi} \int_{-\infty}^{\infty} e^{-i\xi k}\psi_T(\xi)d\xi = \frac{e^{-\alpha k}}{\pi} \int_0^{\infty} e^{-i\xi k}\psi_T(\xi)d\xi. \quad (3.4)$$

More precisely, the call price is determined by substituting (3.3) into (3.4) and performing the required integration. Integration (3.4) is a direct Fourier transform and lends itself to an application of the FFT.

25

Using the Trapezoid rule for the integral in (3.4) and setting $\xi_j = \eta(j-1)$, the value of $C(k)$ is approximated as

$$C_T(k) \approx \frac{e^{-\alpha k}}{2\pi}\left(\psi_T(\xi_1)\eta + e^{-i\xi_N k}\psi_T(\xi_N)\eta\right) + \frac{e^{-\alpha k}}{\pi}\sum_{j=2}^{N-1} e^{-i\xi_j k}\psi_T(\xi_j)\eta. \qquad (3.5)$$

The FFT returns N values of k for a regular spacing size of λ where $log_2 N \in \mathbb{N}$. The FFT requires that $\lambda\eta = \frac{2\pi}{N}$. Hence, the values of k's are:

$$k_u = -b + \lambda(u-1), \qquad \text{for } u = 1, ..., N, \qquad (3.6)$$

which corresponds to log strike prices ranging from $-b$ to b, where $b = \frac{N\lambda}{2}$.

Substituting (3.6) into (3.5) yields

$$C_T(k_u) \approx \frac{e^{-\alpha k_u}}{\pi}\sum_{j=1}^{N} e^{-i\lambda\eta(j-1)(u-1)}e^{ib\xi_j}\psi_T(\xi_j)\eta. \qquad (3.7)$$

The FFT is an efficient algorithm for computing the sum:

$$w(k) = \sum_{j=1}^{N} e^{-i\frac{2\pi}{N}(j-1)(k-1)}x(j), \qquad \text{for } k = 1, \ldots, N,$$

and produces call prices efficiently and accurately. The major advantage of the approach of Carr and Madan (1999) is that it produces call prices for N different strike prices at once. Thus, it facilitates the pracitcal use of calibrating the model to the implied volatilities, which are quoted against strike prices.

It would be interesting to see the performance of FFT implemented to our model. Our numerical example uses $\eta = 0.25$ and $N = 128$, which lead to the log strike price space of $\lambda = 8\pi/128$. The damping coefficient is set at $\alpha=1.5$. Other parameter values are: $\theta = 4.0339$, $\kappa = 10$, $a = 0.5328$, $b = 3.33$, $\sigma = 0.04$, $\rho =$

Strike Price	FFT	Monte Carlo	% Diff.
0.3747	1.0661	1.0658	0.028
0.4559	0.9888	0.9889	-0.01
0.5549	0.8947	0.8958	-0.12
0.6752	0.7802	0.7798	0.05
0.8217	0.6409	0.6413	-0.06
1	0.4713	0.4719	-0.12
1.2170	0.2653	0.2660	-0.26
1.4810	0.0578	0.0583	-0.86
1.8023	0.0011	0.0011	0.94

Table 3.1: Call option prices: FFT vs. Monte Carlo.

0.9, $r = 0.05$, $S_0 = 1.3$, $v_0 = 0.18$, $T = 1$, $F_1 = 1.4954$. We compute the 1 year maturity call options by FFT and compare the results with Monte Carlo simulation with 50,000 sample paths.

The FFT takes around 9 seconds to produce 128 option prices corresponding to different strike prices. The Monte Carlo simulation takes around 50 seconds for each option price. Table 3.1 compares their pricing accuracy. It can be seen that the absolute percentage difference in prices are less than 1% for all cases. If we regard the Monte Carlo price as the benchmark, then this numerical example

confirms that our analytical solution is correct and the FFT is very accurate and efficient.

3.2.2 Implied Volatility
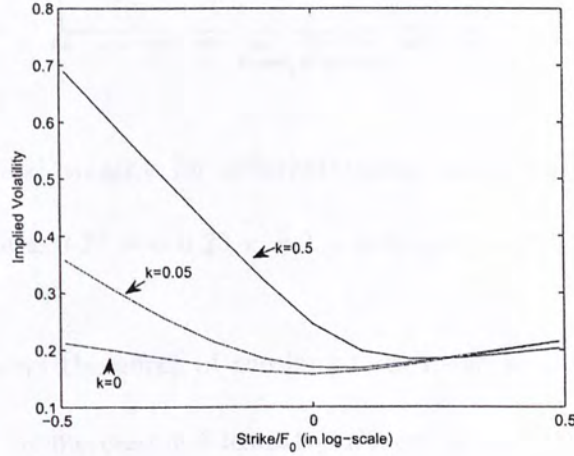
Figure 3.4: Implied volatility for different values of κ. Parameters are $\theta \equiv \kappa \ln(1.2), b = 1, a \equiv 0.2^2, \sigma = 0.35, r = 0, \rho = 0, v_0 = 0.15^2, S_0 = 1$.

The accurate FFT option pricing framework enables us to further investigate the volatility smile implied by the proposed model. Figure 3.4 shows that the left-tail skewness of the volatility smile increases with κ. Consider the case of an exchange rate. If the mean-reversion rate κ represents the force of central bank intervention, then the proposed model implies that the higher the left-tail skewness, the more that the market expects the central bank to intervene. When $\kappa = 0$, it reduces to the Heston model in which a symmetric smile is observed.
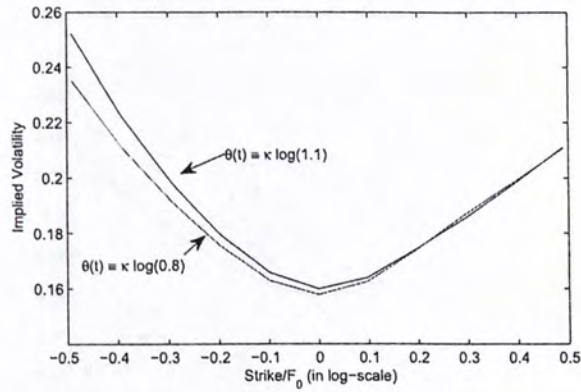
Figure 3.5: Implied volality for different values of θ. Other parameters are: $\kappa = 0.005, b = 1, a \equiv 0.2^2, \sigma = 0.35, r = 0, \rho = 0, v_0 = 0.15^2, S_0 = 1$.

Figure 3.5 shows the effect of the long-term mean level, θ, to the volatility smile. Although the increase in θ leads to an increase in the left-tail of the smile, the effect is much less than that of κ. The overall shape of the smile does not change significantly.

Figure 3.6 shows that a positive correlation raises the right tail and shifts the smile to the left; whereas a negative correlation lowers the right tail, raises the left tail and shifts the curve to the right. This feature is consistent with the Heston model without mean reversion in asset values. Thus, the proposed model maintains some properties of the Heston model. We stress, however, that our model enables option prices to fit the forward price term structure exactly.

29
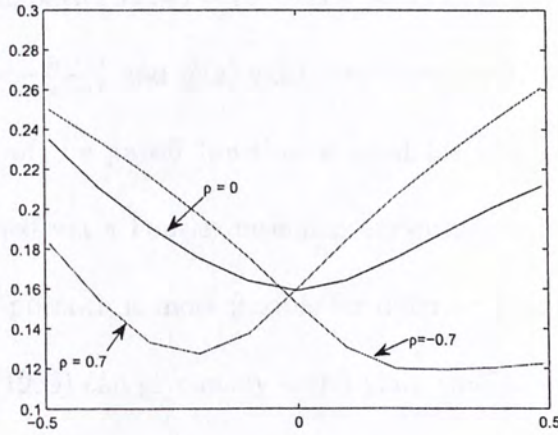
Figure 3.6: Implied volality for different values of ρ. Other parameters are $\theta \equiv 0, \kappa = 0.005, b = 1, a \equiv 0.2^2, \sigma = 0.35, r = 0, v_0 = 0.15^2, S_0 = 1$.

3.2.3 Other Payoff Functions

Lewis (2001) shows that the characteristic function can be used to price European options with any payoff function. Denote $w(x_T)$ to be the payoff function, where $x_T = \log(S_T)$. Assume that $w(x_T)$ is bounded for $|x_T| < \infty$ and its generalized Fourier transform

$$\int_{-\infty}^{\infty} \exp(izx_T)w(x_T)dx_T$$

exists and is regular. Then, the option value is given by:

$$V(S_0) = \frac{e^{-rT}}{2\pi} \int_{i\nu-\infty}^{i\nu+\infty} f(x_0, v, 0; -z)\hat{w}(z)dz,$$

where $x_0 = \log(S_0)$ and $\hat{w}(z)$ is the Fourier transform of the payoff function:

$$\hat{w}(z) = \int_{-\infty}^{\infty} \exp(izx_T)w(x_T)dx_T.$$

30

Consider the call payoff $w(x_T) = (e^{x_T} - K)^+$ as an example. Simple integration shows that $\hat{w}(z) = -\frac{K^{iz+1}}{z^2 - iz}$ and $\hat{w}(z)$ exists in the region $|Im(z)| > 1$. Once the Fourier transform of the payoff function is available, the option price can be numerically obtained via a Fourier inversion algorithm such as FFT. Although the Lewis (2001) approach is more flexible for different payoffs, the approach of Carr and Madan (1999) can give many useful plain vanilla option prices at once. These two approaches serve different needs.

3.3   Trinomial Tree: Exotic Option Pricing

It is most interesting to apply the proposed model to pricing exotic options. The closed-form solutions for European options mainly serve to calibrate the model parameters. The calibrated parameters are then used to price exotic options or structure products for which closed-form pricing formulas are impossible or not readily available. Certainly, Monte Carlo simulation is always a possible alternative valuation approach given the set of calibrated parameters and the stochastic differential equation (3.1). However, simulation is less efficient than a lattice method if the number of factors is small. Our model has only two factors and hence the corresponding tree method is worth considering.

The proposed tree method involves super-calibration to the term structure of forward (futures) prices. Similar to Hull and White (1993), we define a deterministic function g such that $dg = [\theta(t) - \kappa g(t)]dt$ and $g(0) = X_0$. Then, a new

stochastic variable X_t^* is introduced such that $X_t^* = X_t - g(t)$, where the process of X_t is given in (3.1). It is easy to verify that the process of X^* is given by

$$
\begin{aligned}
dX_t^* &= \left[-\kappa X_t^* - \frac{1}{2}v_t\right]dt + \sqrt{v_t}dW_t^{(0)}, \quad X_0^* = 0, \\
dv_t &= (a - bv_t)dt + \sigma\sqrt{v_t}dW_t^{(1)}.
\end{aligned}
\tag{3.8}
$$

Hilliard and Schwartz (1996) propose a combining tree method for a lognormal process with the volatility following an Ornstein-Uhlenbeck process:

$$
du_t = (a - bu_t)dt + \sigma_u u_t dW_t^{(1)}, \quad u_0 = v_0,
$$

where the constant σ_u is the volatility of volatility. As we consider a model consistent with that of Heston (1993), the volatility v_t follows a CIR process. Thus, the process of v_t can be approximated by that of u_t by mathcing the first two moments. A simple calculation shows that

$$
\begin{aligned}
\mathrm{var}(v_T) &= \frac{v_0\sigma^2}{b}(e^{-bT} - e^{-2bT}) + \frac{a\sigma^2}{2b^2}(1 - e^{-bT})^2, \\
\mathrm{var}(u_T) &= u_0\left(e^{(\sigma_u^2 - 2b)T} - e^{-2bT}\right) - \sigma_u^2\frac{a^2(1 - e^{-2bT})}{b^2(\sigma_u^2 - 2b)} + \frac{2a^2(e^{(\sigma_u^2 - 2b)T} - e^{-2bT})}{b(\sigma_u^2 - 2b)} \\
&\quad + \sigma_u^2\left(2au_0 - \frac{2a^2}{b}\right)\left(\frac{e^{-3bT} - e^{-2bT}}{b(\sigma_u^2 - b)} + \frac{e^{(\sigma_u^2 - 2b)T} - e^{-2bT}}{\sigma_u^2(\sigma_u^2 - b)}\right).
\end{aligned}
$$

The value of σ_u^2 can then be solved from the equation $\mathrm{var}(v_T) = \mathrm{var}(u_T)$, with any numerical root finding procedure. Once the σ_u^2 is obtained, we have the following dynamics approximating (3.8):

$$
\begin{aligned}
dX_t^* &= \left[-\kappa X_t^* - \frac{1}{2}u_t\right]dt + \sqrt{u_t}dW_t^{(0)}, \\
du_t &= (a - bu_t)dt + \sigma_u u_t dW_t^{(1)}.
\end{aligned}
\tag{3.9}
$$

The proposed trinomial tree method is based on this approximate dynamic.

32

3.3.1 Sub-tree for the volatility

According to Hilliard and Schwartz (1996), let $y = \frac{1}{\sigma_u} \ln u$, which follows a unit volatility process:

$$dy = \left(\frac{a - be^{y\sigma_u}}{\sigma_u e^{y\sigma_u}} - \frac{\sigma_u}{2} \right) dt + dW_t^{(1)}. \tag{3.10}$$

A trinomial tree is contructed for y. Consider the discrete time points $0 = t_0 < t_1 < ... < t_N = T$, where the time step size $\Delta t_i = t_i - t_{i-1}$ is not necessarily equal for each i. Denote the tree nodes by (i, j), where the time index i ranges from 0 to N and the y-state index j ranges from some $\underline{j_i}$ to some $\overline{j_i}$, and hence $y_{i,j}$ as the process value at the node (i, j). Notice that $y_{0,0} = (\ln u_0)/\sigma_u$ is known. We then set $y_{i,j} = y_{0,0} + j\Delta y_i$, where $\Delta y_i = \sqrt{3\Delta t_i}$.

At the node (i, j), the $y_{i,j}$ can move to $y_{i+1,k+1}$, $y_{i+1,k}$ or $y_{i+1,k-1}$ with probabilities $p_u^{i,j}$, $p_m^{i,j}$ and $p_d^{i,j}$, respectively. From (3.10), it is easy to deduce the expected value of $y(t_{i+1})$ conditional on $y(t_i)$ and the corresponding conditional variance:

$$\mathrm{E}\left[y(t_{i+1})|\, y(t_i)\right] \ := \ y_{i,j} + M_{i,j} = y_{i,j} + \left(\frac{a - be^{y_{i,j}\sigma_u}}{\sigma_u e^{y_{i,j}\sigma_u}} - \frac{\sigma_u}{2} \right) \Delta t_{i+1},$$

$$\mathrm{var}\left[y(t_{i+1})|\, y(t_i)\right] \ := \ V_{i,j} = \Delta t_{i+1}.$$

Matching the first two moments between the diffusion process and the branching process gives

$$p_u^{i,j} \ = \ \frac{V_{i,j}}{2\Delta y_{i+1}^2} + \frac{\alpha^2 + \alpha}{2}, \quad p_d^{i,j} = p_u^{i,j} - \alpha, \quad p_m^{i,j} = 1 - p_u^{i,j} - p_d^{i,j},$$

where

$$\alpha = \frac{j\Delta y_i + M_{i,j} - k\Delta y_{i+1}}{\Delta y_{i+1}}.$$

The central node is thus the k-th node at time t_{i+1}, where $k = \text{round}(\frac{j\Delta y_i + M_{i,j}}{\Delta y_{i+1}})$.

This guarantees that all the branching probabilities are non-negative. The tree for the process of u_t is then obtained as $u_t = e^{y_t \sigma_u}$. Thus, the value of u_t is always positive even though the value of y can reach negative.

3.3.2 Sub-tree for the asset

The tree for X_t^* is considered next. Let $H(X_t^*, u_t) = X^*/\sqrt{u_t}$. Applying Itô's lemma on H yields,

$$dH = m_H dt + \sigma_H dW_H,$$

where

$$
\begin{aligned}
m_H &= \left(\frac{b}{2} + \frac{3\sigma_u^2}{8} - \kappa - \frac{au^{-1}}{2} \right) H - \frac{1}{2}(u^{\frac{1}{2}} + \rho\sigma_u), \\
\sigma_H &= \left(1 - \rho\sigma_u H + (\frac{1}{2}\sigma_u H)^2 \right)^{\frac{1}{2}}, \quad E(dW_H dW_t^{(1)}) = \frac{\rho - \frac{1}{2}\sigma_u H}{\sigma_H} dt.
\end{aligned}
$$

We suppose for the moment that the correlation between dW_H and $dW_t^{(1)}$ is zero. This should not be true because the constant ρ cannot make the correlation $\frac{\rho - \sigma_u H/2}{\sigma_H}$ zero for all time points. However, the tree incorporating the correlation that will be developed in the next subsection requires a tree with zero correlation as an input.

Consider the transformation:

$$Q = \frac{2}{\sigma_u} \ln \left(\frac{1}{2}\sigma_u H - \rho + \sigma_H \right). \tag{3.11}$$

An application of Itô's lemma shows that

$$dQ = F_2(u, Q)dt + dW_H, \tag{3.12}$$

where

$$F_2(u, Q) = \frac{m_H}{\sigma_H} + \frac{1}{2}\frac{\partial^2 Q}{\partial H^2}\sigma_H^2 = \frac{\left(\frac{b}{2} + \frac{\sigma_u^2}{4} - \kappa - \frac{au^{-1}}{2}\right)H - \frac{1}{4}(2u^{\frac{1}{2}} + \rho\sigma_u)}{\left(1 - \rho\sigma_u H + (\frac{1}{2}\sigma_u H)^2\right)^{\frac{1}{2}}}.$$

As (3.11) implies that

$$H = F_1(Q) = \sigma_u^{-1}\left[2\rho - (1 - \rho^2)e^{-\frac{\sigma_u}{2}Q} + e^{\frac{\sigma_u}{2}Q}\right],$$

we have

$$F_2(u, Q) = \frac{\left(\frac{b}{2} + \frac{\sigma_u^2}{4} - \kappa - \frac{au^{-1}}{2}\right)F_1(Q) - \frac{1}{4}(2u^{\frac{1}{2}} + \rho\sigma_u)}{\left(1 - \rho\sigma_u F_1(Q) + (\frac{1}{2}\sigma_u F_1(Q))^2\right)^{\frac{1}{2}}}.$$

Hence, Q follows a unit volatility process. The corresponding value of X^* is then given by the inverse transform:

$$X^* = u^{\frac{1}{2}}F_1(Q). \tag{3.13}$$

Given the discrete time points $0 = t_0 < t_1 < \ldots < t_N = T$, the tree for the process of Q is investigated. Other than the time space and the y-space, the tree should be expanded to incorporate the Q-space. Hence, the tree nodes can be labeled as (i, j, ℓ) where the additional Q-space index ℓ ranges from some $\underline{\ell_i}$ to some $\overline{\ell_i}$. Note that the ranges for i and j have been specified early. Hence, we have $Q_{i,j,\ell}$ representing the value of Q at the node (i, j, ℓ) where $Q_{i,j,\ell} = Q_{0,0,0} + \ell\Delta Q_i$. The initial value $Q_{0,0,0}$ is a known quantity and $\Delta Q_i = \sqrt{3\Delta t_i}$. The conditional

35

mean and variance of $Q(t_{i+1})$ can be easily deduced from (3.12):

$$\mathrm{E}\left[Q(t_{i+1})|Q(t_i),u(t_i)\right] \;\; := \;\; Q_{i,j,\ell} + N_{i,j,\ell} = Q_{i,j,\ell} + [F_2(u_{i,j,\ell},Q_{i,j,\ell})]\Delta t_{i+1}$$

$$\mathrm{var}\left[Q(t_{i+1})|Q(t_i),u(t_i)\right] \;\; := \;\; V_{i,j,\ell} = \Delta t_{i+1} \tag{3.14}$$

From time point t_i to time point t_{i+1}, there are nine possibilities for the value of Q at time t_{i+1} given that $Q = Q_{i,j,\ell}$ at time t_i. Specifically, the value of $Q_{i,j,\ell}$ can move up to $Q_{i+1,k+1,n+1}$ or $Q_{i+1,k,n+1}$ or $Q_{i,k-1,n+1}$ with total probability $q_u^{i,j,\ell}$, or move down to $Q_{i+1,k+1,n-1}$ or $Q_{i+1,k,n-1}$ or $Q_{i+1,k-1,n-1}$ with total probability $q_d^{i,j,\ell}$, or move to $Q_{i+1,k+1,n}$ or $Q_{i+1,k,n}$ or $Q_{i+1,k-1,n}$ with total probability $q_m^{i,j,\ell}$. These probabilities can be derived by matching the mean and variance between the diffusion process (3.12) with the corresponding branching process. A simple calculation, similar to that of Hull and White (1993), shows that

$$q_u^{i,j,\ell} \;\; = \;\; \frac{V_{i,j,\ell}}{2\Delta Q_{i+1}^2} + \frac{\beta^2+\beta}{2}, \quad q_d^{i,j,\ell} = q_u^{i,j,\ell} - \beta, \quad q_m^{i,j,\ell} = 1 - q_u^{i,j,\ell} - q_d^{i,j,\ell},$$

where

$$\beta = \frac{\ell \Delta Q_i + N_{i,j,\ell} - n \Delta Q_{i+1}}{\Delta Q_{i+1}}, \quad n = \mathrm{round}\left(\frac{\ell \Delta Q_i + N_{i,j,\ell}}{\Delta Q_{i+1}}\right).$$

In this two-dimensional trinomial tree, there are nine branches emanating from the (i,j,ℓ) node. The probabilities associated with the nine branches are:

<div align="center">

Q-Move

</div>

		Lower	Middle	Upper
	Upper	$p_u^{i,j} q_d^{i,j,\ell}$	$p_u^{i,j} q_m^{i,j,\ell}$	$p_u^{i,j} q_u^{i,j,\ell}$
u-Move	Middle	$p_m^{i,j} q_d^{i,j,\ell}$	$p_m^{i,j} q_m^{i,j,\ell}$	$p_m^{i,j} q_u^{i,j,\ell}$
	Lower	$p_d^{i,j} q_d^{i,j,\ell}$	$p_d^{i,j} q_m^{i,j,\ell}$	$p_d^{i,j} q_u^{i,j,\ell}$

3.3.3 Non-zero Correlation

As the tree for X_t^* developed in the last subsection assumes zero correlation between dW_H and $dW^{(1)}$, this subsection relaxes that assumption. We recall that

$$\mathrm{E}[dW_H dW_t^{(1)}] = \left(\frac{\rho - \frac{1}{2}\sigma_u H}{\sigma_H}\right) dt = \frac{\rho - \frac{1}{2}\sigma_u F_1(Q)}{\left(1 - \rho\sigma_u F_1(Q) + (\frac{1}{2}\sigma_u F_1(Q))^2\right)^{\frac{1}{2}}} dt. \quad (3.15)$$

Thus, the correlation at each node depends on the value of Q at that node and the correlation is non-zero in general for a constant ρ.

Similar to Hilliard and Schwartz (1996), we define

$$r_{i,j,\ell} = \frac{\rho - \frac{1}{2}\sigma_u F_1(Q_{i,j,\ell})}{\left(1 - \rho\sigma_u F_1(Q_{i,j,\ell}) + (\frac{1}{2}\sigma_u F_1(Q_{i,j,\ell}))^2\right)^{\frac{1}{2}}},$$

which measures the correlation coefficient between $\Delta W_H(t_{i+1})$ and $\Delta W^{(1)}(t_{i+1})$ at the node (i, j, ℓ). If $r_{i,j,\ell}$ is indeed zero, then no adjustment is required and the tree developed in the last subsection is applied.

<div align="center">Q-Move</div>

		Lower	Middle	Upper
	Upper	$p_u^{i,j} q_d^{i,j,\ell} - \varepsilon$	$p_u^{i,j} q_m^{i,j,\ell} - 4\varepsilon$	$p_u^{i,j} q_u^{i,j,\ell} + 5\varepsilon$
u-Move	Middle	$p_m^{i,j} q_d^{i,j,\ell} - 4\varepsilon$	$p_m^{i,j} q_m^{i,j,\ell} + 8\varepsilon$	$p_m^{i,j} q_u^{i,j,\ell} - 4\varepsilon$
	Lower	$p_d^{i,j} q_d^{i,j,\ell} + 5\varepsilon$	$p_d^{i,j} q_m^{i,j,\ell} - 4\varepsilon$	$p_d^{i,j} q_u^{i,j,\ell} - \varepsilon$

<div align="center">Table 3.2: Adjustment with positive correlation</div>

If the correlation $r_{i,j,\ell}$ is positive, then the adjustment corresponding to Table 3.2 can be made to obtain a set of transition probabilities, $p(i + 1, k, n|i, j, \ell)$,

$$Q\text{-Move}$$

		Lower	Middle	Upper
	Upper	$p_u^{i,j}q_d^{i,j,\ell} + 5\varepsilon$	$p_u^{i,j}q_m^{i,j,\ell} - 4\varepsilon$	$p_u^{i,j}q_u^{i,j,\ell} - \varepsilon$
u-Move	Middle	$p_m^{i,j}q_d^{i,j,\ell} - 4\varepsilon$	$p_m^{i,j}q_m^{i,j,\ell} + 8\varepsilon$	$p_m^{i,j}q_u^{i,j,\ell} - 4\varepsilon$
	Lower	$p_d^{i,j}q_d^{i,j,\ell} - \varepsilon$	$p_d^{i,j}q_m^{i,j,\ell} - 4\varepsilon$	$p_d^{i,j}q_u^{i,j,\ell} + 5\varepsilon$

Table 3.3: Adjustment with negative correlation

which represents the probability of moving from the node (i, j, ℓ) to the node $(i + 1, k, n)$. This adjustment does not change the means and variances of the unconditional movements in u and Q. Alternatively, if $r_{i,j,\ell}$ is negative, then the adjustment corresponding to Table 3.3 is applied to the transition probabilities. In both Tables 3.2 and 3.3, $\varepsilon = r_{i,j,\ell}/36$. Once the two-dimensional tree of (Q, u) is available, it can be transformed back to that of (X^*, u) by using the inverse transformation (3.13).

3.3.4 Calibration to Future prices

Suppose that future prices with maturities t_i are observed at $t = 0$. We now explain how $g_i = g(t_i)$ can be calibrated to the observed future prices. Note that $g_0 = X_0 = \ln S_0$. The future price with maturity t_i has the expression

$$F_{t_i} = E(S_{t_i} | \mathcal{F}_0) = E\left[e^{X_{t_i}^* + g_i} \middle| \mathcal{F}_0 \right], \tag{3.16}$$

where $\mathcal{F}_t$ is the market information (or filtration) accumulated up to time t. Formula (3.16) implies that

$$g_i = \ln \left(\frac{1}{F_{t_i}} E \left[e^{X_{t_i}^*} \,\middle|\, \mathcal{F}_0 \right] \right), \tag{3.17}$$

where the expectation in right-hand side can be effectively computed with the (X^*, u)-tree for all $i = 1, \cdots, N$. After $g_1, \cdots, g_N$ have been calculated from (3.17), the (X, u)-tree is established by setting $X_{i,j,\ell} = X_{i,j,\ell}^* + g_i$ with the transition probabilities $p(i+1, k, n|i, j, \ell)$ obtained in the last subsection.

3.3.5 Numerical Examples

The accuracy and efficiency of the proposed lattice approach are examined using numerical examples. As the numerical scheme is designed for pricing exotic options with no closed-form solution available, the examples use barrier and American options. The prices obtained from Monte Carlo simulation are regarded as benchmarks for the accuracy of the proposed scheme, where the simulation is based on the dynamics (3.1). This simulation of barrier options is clear but that of American options requires the least-squared regression for estimating the conditional expectation of the option value of continuation. The regression is based on an order three polynomial. The Monte Carlo simulation uses 50,000 sample paths and a time-step of $1/500$.

The numerical results are displayed in Table 3.4. The percentage differences between the lattice approach and the simulation are consistently less than 1%

for both barrier and American options. As the lattice approach is constructed from the approximate processes (3.9), the numerical results indicate that the approximation does not lead to significant error for path-dependent option pricing. However, the lattice approach is much more efficient than the Monte Carlo simulation because it takes less than 18 seconds to compute an option price, regardless of whether it is a barrier or an American option, but the Monte Carlo simulation takes more than 2 minutes. Although the simulation may be improved by using some variance reduction techniques, it is still impossible to price an exotic option within 20 seconds with the MRSV model. Another nice feature of the lattice approach is that it allows calibration to future prices within the tree building procedure.

	Down and Out Call Option			American Call Option		
Strike	Monte Carlo	Lattice	Abs Diff.	Monte Carlo	Lattice	Abs Diff.
0.2	0.7903	0.7854	0.62%	0.9416	0.9417	0.01%
0.3	0.6908	0.6866	0.61%	0.8417	0.8417	0.06%
0.4	0.5916	0.5877	0.66%	0.7417	0.7437	0.27%
0.5	0.4920	0.4927	0.14%	0.6425	0.6417	0.12%
0.6	0.3923	0.3901	0.56%	0.5425	0.5417	0.15%
0.7	0.2931	0.2913	0.61%	0.4416	0.4417	0.03%
0.8	0.1943	0.1928	0.77%	0.3417	0.3418	0.02%

Table 3.4: Option price comparison between simulation and proposed trinomial tree method. The value of the barrier is set to 0.7 for the barrier option. The parameters are $\theta=0$, $\kappa=10$, $a=2$, $b=10$, $\sigma=0.2$, $\sigma_u=0.445$, $\rho=0.8$, $r=0$, $S_0=1$, $v_0=0.2$ and $T=1$.

Chapter 4

Multiscale Stochastic Volatility

In this chapter, we detail the multiscale SV model with mean reversion underlying process. Specifically, we derive the partial differential equation (PDE) for European option. An asymptotic solution to the PDE is then established by means of singular perturbation technique of Fouque *et al.* (2003b). The accuracy of the analytic approximation is presented in the last part.

4.1 Model Settings

Let F_t denote the underlying exchange rate at time t. Under the risk neutral probability measure,

$$
\begin{aligned}
\frac{dF_t}{F_t} &= [k(\log \bar{F} - \log F_t) + r - r_f]dt + f(Y_t, Z_t)dW_t^{(0)*}, \\
dY_t &= \left[\frac{1}{\epsilon}(m - Y_t) - \frac{\nu\sqrt{2}}{\sqrt{\epsilon}}\Lambda(Y_t, Z_t)\right]dt + \frac{\nu\sqrt{2}}{\sqrt{\epsilon}}dW_t^{(1)*}, \\
dZ_t &= \left[\delta c(Z_t) - \sqrt{\delta}g(Z_t)\Gamma(Y_t, Z_t)\right]dt + \sqrt{\delta}g(Z_t)dW_t^{(2)*},
\end{aligned} \tag{4.1}
$$

where ν, m, ϵ, and δ are constant parameters, r is the domestic interest rate, r_f is the foreign interest rate, $W_t^{(0)}$, $W_t^{(1)}$, and $W_t^{(2)}$ are Wiener processes, $f(Y, Z)$ is a positive function representing the volatility of the stock and Λ and Γ are the functional forms reflect the risk-neutral measure that used by the market.

The first factor Y_t represents fast scale volatility factor driving the volatility. It is a fast mean reverting diffusion process corresponding to a Gaussian Ornstein-Uhlenbeck process. $\frac{1}{\epsilon}$ is the rate of mean reversion of this process, with $\epsilon > 0$ being a small parameter which corresponds to the time scale of this process.

The second factor Z_t driving the volatility is a slowly varying diffusion process. When we explicitly specify the functions: $c(Z_t) = m_2 - Z_t$ and $\sqrt{\delta}g(Z_t) = \beta_2 Z_t^p$, we recognize that δ is the mean-reverting rate for the process of Z_t. However, we will see shortly that the functional forms of $c(Z)$ and $g(Z)$ do not affect the structure of option pricing formulas if both δ and ϵ are small parameters. This assumption is supported by empirical evidence that Alizadeh et al. (2002) observed $\delta \sim 0.05$ and Fouque et al. (2000) obtained $\epsilon \sim 0.005$. When both ϵ and δ are small, the stochastic variable Y_t stands for a fast mean-reverting factor and the stochastic variable Z_t is a persistent factor. We allow a general correlation structure among three Wiener processes $W_t^{(0)}$, $W_t^{(1)}$, and $W_t^{(2)}$ so that

$$\begin{pmatrix} W^{(0)} \\ W^{(1)} \\ W^{(2)} \end{pmatrix} = \begin{pmatrix} 1 & 0 & 0 \\ \rho_1 & \sqrt{1 - \rho_1^2} & 0 \\ \rho_2 & \widetilde{\rho}_{12} & \sqrt{1 - \rho_2^2 - \widetilde{\rho}_{12}^2} \end{pmatrix} \mathbf{W}_t, \qquad (4.2)$$

where $\mathbf{W}_t$ is a standard independent three-dimensional Brownian motion, and

the constant coefficients ρ_1, ρ_2, and $\widetilde{\rho}_{12}$ satisfy $|\rho_1| < 1$ and $\rho_2^2 + \widetilde{\rho}_{12}^2 < 1$.

4.2 Pricing

Let $P^{\epsilon,\delta}(t, F, y, z)$ be the price function for a European call option. The corresponding payoff function is denoted as $\widehat{H}(F) = F - K$. Denote $E^{\mathbb{Q}}\{\}$ be the expectation with respect to the risk-neutral measure described above, the price of a European option with payoff function $H(F)$ is given by:

$$P^{\epsilon,\delta}(t, F, y, z) = E^{\mathbb{Q}}\left\{ e^{-r(T-t)}\widehat{H}(F_T) \Big| F_t = F, Y_t = y, Z_t = z \right\},$$

where $\mathbb{Q}$ is the risk-neutral measure under which the processes of (4.1) are defined. By application of the Feynman-Kac formula, we obtain $P^{\epsilon,\delta}(t, F, y, z)$ as the solution of the partial differential equation (PDE) with a terminal boundary value problem

$$\mathcal{L}^{\epsilon,\delta} P_t^{\epsilon,\delta} = 0, \quad 0 \leq t < T,$$

$$P^{\epsilon,\delta}(T, L_T, y, z) = H(L_T) = e^{L_T e^{-kT}} - K, \tag{4.3}$$

where

$$L_t = e^{kt}\ln F_t, \quad \theta = k\log\bar{F} + r - r_f$$

$$\mathcal{L}^{\epsilon,\delta} = \frac{1}{\epsilon}\mathcal{L}_0 + \frac{1}{\sqrt{\epsilon}}\mathcal{L}_1 + \mathcal{L}_2 + \sqrt{\delta}\mathcal{M}_1 + \delta\mathcal{M}_2 + \sqrt{\frac{\delta}{\epsilon}}\mathcal{M}_3,$$

$$\mathcal{L}_0 = (m - y)\frac{\partial}{\partial y} + \nu^2\frac{\partial^2}{\partial y^2},$$

$$\mathcal{L}_1 = \nu\sqrt{2}\rho_1 f(y, z)e^{kt}\frac{\partial^2}{\partial L\partial y} - \nu\sqrt{2}\Lambda(y, z)\frac{\partial}{\partial y},$$

44

$$\mathcal{L}_2 = \frac{\partial}{\partial t} + \frac{1}{2}f(y,z)^2 e^{2kt}\frac{\partial^2}{\partial L^2} + \left(\theta e^{kt} - \frac{f(y,z)^2}{2}e^{kt}\right)\frac{\partial}{\partial L} - r\cdot, \quad (4.4)$$

$$\mathcal{M}_1 = -g(z)\Gamma(y,z)\frac{\partial}{\partial z} + \rho_2 g(z)f(y,z)e^{kt}\frac{\partial^2}{\partial L\partial z},$$

$$\mathcal{M}_2 = c(z)\frac{\partial}{\partial z} + \frac{1}{2}g(z)^2\frac{\partial^2}{\partial z^2},$$

$$\mathcal{M}_3 = \nu\sqrt{2}\left(\rho_1\rho_2 + \tilde{\rho}_{12}\sqrt{1-\rho_1^2}\right)g(z)\frac{\partial^2}{\partial y\partial z}.$$

The governing equation is the consequence of the Feynman-Kac formula that is followed by the transformation of variables.

In this section, we give a formal derivation of the price approximation by solving (4.3) in asymptotic expansions when δ and ϵ are small independent parameters. Consider the pricing formula of the form

$$P = P_0 + \sqrt{\epsilon}P_{1,0} + \sqrt{\delta}P_{0,1} + \sqrt{\epsilon\delta}P_{1,1} + \epsilon P_{2,0} + \delta P_{0,2} + \cdots, \quad (4.5)$$

where P_0 (or $P_{0,0}$) and $P_{i,j}$ are functions of (t, L, y, z) that will be solved in succession until certain accuracy is attained.

We insert the expansion (4.5) in the equation (4.3) and find that equations associated with the first two leading terms which are respectively $\mathcal{O}(1/\epsilon)$ terms and $\mathcal{O}(1/\sqrt{\epsilon})$ terms. We end up with

$$\mathcal{L}_0 P_0 = 0,$$

$$\mathcal{L}_0 P_{1,0} + \mathcal{L}_1 P_0 = 0.$$

These are two ordinary differential equations in y. P_0 can be confirmed to be a function that is independent of y and $P_{1,0}$ is also a function that is independent

of y. Continuing the process, we obtain the $\mathcal{O}(1)$ term as

$$\mathcal{L}_0 P_{2,0} + \mathcal{L}_1 P_{1,0} + \mathcal{L}_2 P_0 = 0 \Rightarrow \mathcal{L}_0 P_{2,0} + \mathcal{L}_2 P_0 = 0. \qquad (4.6)$$

Given the function P_0, equation (4.6) is a Poisson equation on $P_{2,0}$. There is a unique solution at most polynomially going to infinity if

$$E_y(\mathcal{L}_2 P_0) = 0, \quad y \sim \mathcal{N}(m, \nu^2),$$

where the distribution of y is the invariant distribution of the operator $\mathcal{L}_0$. This fact is known as the Fredholm solvability for Poisson equations. As P_0 is a function that is independent of y, the expectation only takes effect on the operator $\mathcal{L}_2$ through the function $f(y, z)$. Thus,

$$E_y(\mathcal{L}_2 P_0) = E_y(\mathcal{L}_2) P_0 = 0, \quad 0 \le t < T, \qquad (4.7)$$

$$P_0(T, L_T) = H(L_T).$$

A more explicit expression of (4.7) can be obtained through denoting

$$E_y(f(y, z)^2) = \overline{\sigma}(z)^2, \quad y \sim \mathcal{N}(m, \nu^2). \qquad (4.8)$$

It follows that the $E_y(\mathcal{L}_2)$ in (4.7) is the following operator with a volatility $\overline{\sigma}(z)$ that is independent of y. Hence, we define

$$\mathcal{L}_{BS}^z := E_y(\mathcal{L}_2) = \frac{\partial}{\partial t} + \frac{1}{2}\overline{\sigma}(z)^2 e^{2kt}\frac{\partial^2}{\partial L^2} + \left(\theta e^{kt} - \frac{\overline{\sigma}(z)^2 e^{kt}}{2}\right)\frac{\partial}{\partial L} - r \cdot. \qquad (4.9)$$

In fact, the parameter $\overline{\sigma}(z)$ is the short-term realized volatility of the underlying value because the distribution of y is the invariant distribution of Y_t, with Z_t

46

being fixed. An explanation of this interpretation is provided by Fouque et al. (2003b). This observation together with (4.7) leads to the following consequence.

The zeroth order approximation for the call option is the pricing formula of that option corresponding to operator $\mathcal{L}_{BS}^{z}$ in (4.9) with a short-term volatility, $\overline{\sigma}(z)$, defined in (4.8).

$$P_0 = \hat{L} e^{-r(T-t)} N(d_1) - K e^{-r(T-t)} N(d_2), \tag{4.10}$$

where

$$\hat{L} = e^{L_t e^{-kT} + \frac{(\theta - \frac{\overline{\sigma}(z)^2}{2})}{k}(1-e^{-k(T-t)}) + \frac{v^2}{2}} = F_t e^{-k(T-t)} e^{\frac{(\theta - \frac{\overline{\sigma}(z)^2}{2})}{k}(1-e^{-k(T-t)}) + \frac{v^2}{2}},$$

$$v^2 = \frac{\overline{\sigma}(z)^2 e^{-2k(T-t)}}{2k}(e^{2k(T-t)} - 1),$$

$$d_1 = \frac{\ln(\frac{\hat{L}}{K}) + \frac{v^2}{2}}{v}, \quad d_2 = d_1 - v,$$

In the following, we use perturbation methods to derive the first order correction term by separating it into two parts: fast timesale and slow timescale asymptotics. The fast (slow) timescale asymptotic solution corresponds to the correction term due to the fast (slow) timescale factor.

Consider $\mathcal{O}(\sqrt{\epsilon})$ terms in (4.3),

$$\mathcal{L}_0 P_{3,0} + \mathcal{L}_1 P_{2,0} + \mathcal{L}_2 P_{1,0} = 0,$$

that lead to the result

$$E_y(\mathcal{L}_1 P_{2,0}) + E_y(\mathcal{L}_2) P_{1,0} = 0,$$

after applying the Fredholm solvability and recognizing $P_{1,0}$ to be independent of y. To solve $P_{1,0}$ from the above equation, we express $P_{2,0}$ in terms of P_0 by

equation (4.6) to yield

$$\mathcal{L}_{BS}^z P_{1,0} = E_y(\mathcal{L}_1 \mathcal{L}_0^{-1} \mathcal{L}_2 P_0), \quad 0 \leq t < T, \tag{4.11}$$

$$P_{1,0}(T, L_T, z) = 0.$$

The right-hand side of (4.11) is a known quantity as P_0 has been obtained by the early steps. Therefore, the PDE (4.11) becomes a equation for European call options with a source term — the function in the right hand side of (4.11). By recognizing that $\mathcal{L}_2 P_0 = (\mathcal{L}_2 - E_y(\mathcal{L}_2)) P_0$ so that

$$\mathcal{L}_2 P_0 = \frac{f(y,z)^2 - \bar{\sigma}(z)^2}{2} \left(-e^{kt} \frac{\partial}{\partial L} + e^{2kt} \frac{\partial^2}{\partial L^2} \right) P_0.$$

Let $\phi(y,z)$ be the solution of the ODE:

$$\mathcal{L}_0 \phi = f(y,z)^2 - \bar{\sigma}(z)^2.$$

As the term $\mathcal{L}_2 P_0$ depends on y only through $f(y,z)$, we have

$$\mathcal{L}_0^{-1} \mathcal{L}_2 P_0 = \frac{\phi(y,z)}{2} \left(-e^{kt} \frac{\partial}{\partial L} + e^{2kt} \frac{\partial^2}{\partial L^2} \right) P_0,$$

which implies that

$$E_y(\mathcal{L}_1 \mathcal{L}_0^{-1} \mathcal{L}_2 P_0) = (V_3(z)(e^{3kt} \frac{\partial^3}{\partial L^3} - e^{2kt} \frac{\partial^2}{\partial L^2}) - V_2(z)(e^{2kt} \frac{\partial^2}{\partial L^2} - e^{kt} \frac{\partial}{\partial L}))P_0,$$

where

$$V_2(z) = \frac{\nu}{\sqrt{2}} E_y \left(\frac{\partial \phi(y,z)}{\partial y} \Lambda(y,z) \right) \quad \text{and} \quad V_3(z) = \frac{\rho_1 \nu}{\sqrt{2}} E_y \left(\frac{\partial \phi(y,z)}{\partial y} f(y,z) \right),$$

$V_2(z)$ and $V_3(z)$ are effective parameters to be calibrated. It is clear that functions of the form, $\partial^n P_0 / \partial L^n$, are homogeneous solutions to the PDE (4.11),

i.e.,

$$\mathcal{L}_{BS}^z \left[\frac{\partial^n P_0}{\partial L^n} \right] = 0.$$

Hence, the source term is actually a linear combination of homogeneous solutions of (4.11).

To obtain $P_{1,0}$ analytically, we solve (4.11) in closed form.

Theorem 4.2.1. Consider the PDE:

$$\mathcal{L}_{BS}^z F = \sum_{i=1}^n k_i(t, z) G_i(t, L_t, z), \ 0 \le t < T,$$
$$F(T, L_T, z) = 0,$$

If $\mathcal{L}_{BS}^z G_i = 0$ for all $i = 1, 2, \cdots, n$, then the solution is given by

$$F(t, L_t, z) = -\sum_{i=1}^n \left[\int_t^T k_i(\theta, z) d\theta \right] G_i(t, L_t, z),$$

A direct consequence of Theorem 4.2.1 is that

$$\begin{aligned}
P_{1,0} &= -[V_3(z)(\frac{e^{3kT} - e^{3kt}}{3k} \frac{\partial^3}{\partial L^3} - \frac{e^{2kT} - e^{2kt}}{2k} \frac{\partial^2}{\partial L^2}) \\
&\quad -V_2(z)(\frac{e^{2kT} - e^{2kt}}{2k} \frac{\partial^2}{\partial L^2} - \frac{e^{kT} - e^{kt}}{k} \frac{\partial}{\partial L})]P_0,
\end{aligned} \tag{4.12}$$

Here also explain the necessity of transform F_t into L_t so that solution of (4.11) can be solved by Theorem 4.2.1.

By collecting $\mathcal{O}(\sqrt{\delta}/\epsilon)$ terms, we have

$$\mathcal{L}_0 P_{0,1} = 0.$$

This implies $P_{0,1}$ does not depend of y. Collect $\mathcal{O}(\sqrt{\delta/\epsilon})$ terms:

$$\mathcal{L}_0 P_{1,1} + \mathcal{L}_1 P_{0,1} + \mathcal{M}_3 V_0 = 0.$$

49

We ensure that

$$\mathcal{L}_0 P_{1,1} = 0,$$

because P_0 and $P_{1,0}$ are functions that are independent of y and both operators of $\mathcal{L}_1$ and $\mathcal{M}_3$ involve a y differential. Thus, $P_{1,1}$ also does not depend on y.

To determine the slowscale correction term $\sqrt{\delta} P_{0,1}$, collect $\mathcal{O}(\sqrt{\delta})$ terms from equation (4.3):

$$\mathcal{L}_0 P_{2,1} + \mathcal{L}_1 P_{1,1} + \mathcal{L}_2 P_{0,1} + \mathcal{M}_1 P_0 + \mathcal{M}_3 P_{1,0} = 0.$$

As $P_{1,1}$ and $P_{1,0}$ are functions that are independent of y, the above governing equation is reduced to

$$\mathcal{L}_0 P_{2,1} + \mathcal{L}_2 P_{0,1} + \mathcal{M}_1 P_0 = 0,$$

which is a Poisson equation on $P_{2,1}$ given the functions $P_{0,1}$ and P_0. Applying Fredholm solvability and recognizing $P_{0,1}$ to be a function independent of y, we obtain a PDE for the slowscale correction term:

$$\mathcal{L}_{BS}^z P_{0,1} = -E_y(\mathcal{M}_1) P_0, \quad 0 < l < T, \tag{4.13}$$

$$P_{0,1}|_{t=T} = 0.$$

It can be shown that the source term of PDE (4.13) is:

$$-E_y(\mathcal{M}_1) P_0 = 2 \frac{V_0(z)}{\overline{\sigma}(z)} \frac{\partial P_0}{\partial \overline{\sigma}} - 2 \frac{V_1(z)}{\overline{\sigma}(z)} e^{kt} \frac{\partial}{\partial L} \left(\frac{\partial P_0}{\partial \overline{\sigma}} \right), \tag{4.14}$$

where

$$V_0(z) = \frac{1}{2} g(z) \overline{\sigma}(z) \frac{\partial \overline{\sigma}(z)}{\partial z} E_y \left[\Gamma(y, z) \right]$$

$$V_1(z) = \frac{1}{2} g(z) \rho_2 \overline{\sigma}(z) \frac{\partial \overline{\sigma}(z)}{\partial z} E_y \left[f(y, z) \right].$$

$V_0(z)$ and $V_1(z)$ are effective parameters to be calibrated, and $\partial P_0/\partial \bar{\sigma}$ is known as the vega of the option. Hence, the first order slow timescale correction is related to the vega and delta-vega of the option.

To solve (4.13) analytically, we connect the vega and delta-vega to homogeneous solutions of (4.13) so that Theorem 4.2.1 can be applied. Consider that P_0 satisfies

$$\mathcal{L}_{BS}^z P_0 = 0.$$

By differentiating both sides with respect to $\bar{\sigma}(z)$, we have

$$\mathcal{L}_{BS}^z \left[\frac{\partial P_0}{\partial \bar{\sigma}} \right] = -\bar{\sigma} \left(e^{2kt} \frac{\partial^2}{\partial L^2} - e^{kt} \frac{\partial}{\partial L} \right) P_0.$$

Therefore, the option vega is the unique solution to the following PDE:

$$\mathcal{L}_{BS}^z u = -\bar{\sigma} \left(e^{2kt} \frac{\partial^2}{\partial L^2} - e^{kt} \frac{\partial}{\partial L} \right) P_0, \tag{4.15}$$

$$u(T, L, z) = \frac{\partial P_0}{\partial \bar{\sigma}} \bigg|_{t=T}.$$

By verifying that $\bar{\sigma}(\frac{e^{2kT}-e^{2kt}}{2k}) \frac{\partial^2 P_0}{\partial L^2} - \bar{\sigma}(\frac{e^{kT}-e^{kt}}{k}) \frac{\partial P_0}{\partial L}$ satisfies the governing equation of (4.15), we conclude that

$$\frac{\partial P_0}{\partial \bar{\sigma}} = u = \bar{\sigma}(\frac{e^{2kT} - e^{2kt}}{2k}) \frac{\partial^2 P_0}{\partial L^2} - \bar{\sigma}(\frac{e^{kT} - e^{kt}}{k}) \frac{\partial P_0}{\partial L} + u_h, \tag{4.16}$$

where u_h is a homogeneous solution, i.e., $\mathcal{L}_{BS}^z u_h = 0$.

Therefore, the vega is a linear combination of homogeneous solutions with time-dependent coefficients. The same conclusion applies to the delta-vega because the x−differential of a homogeneous solution is also a homogeneous solution due to the linearity of the operator $\mathcal{L}_{BS}^z$ in x.

51

Substituting (4.16) into (4.14) yields

$$
\begin{aligned}
-E_y(\mathcal{M}_1)P_0 &= 2\frac{V_0(z)}{\overline{\sigma}(z)}\frac{\partial P_0}{\partial \overline{\sigma}} - 2\frac{V_1(z)}{\overline{\sigma}(z)}e^{kt}\frac{\partial}{\partial L}\left(\frac{\partial P_0}{\partial \overline{\sigma}}\right) \\
&= \left(\frac{e^{2kT}-e^{2kt}}{k}\right)\left(V_0(z)\frac{\partial^2 P_0}{\partial L^2} - e^{kt}V_1(z)\frac{\partial^3 P_0}{\partial L^3}\right) \\
&\quad -2\left(\frac{e^{kT}-e^{kt}}{k}\right)\left(V_0(z)\frac{\partial P_0}{\partial L} - e^{kt}V_1(z)\frac{\partial^2 P_0}{\partial L^2}\right) \\
&\quad +2\left[\frac{V_0(z)}{\overline{\sigma}(z)}u_h - e^{kt}\frac{V_1(z)}{\overline{\sigma}(z)}\frac{\partial u_h}{\partial L}\right].
\end{aligned}
\tag{4.17}
$$

By Theorem 4.2.1, we have

$$
\begin{aligned}
P_{0,1} &= -V_0(z)\left(\frac{(T-t)e^{2kT}-\frac{1}{2k}(e^{2kT}-e^{2kt})}{k}\frac{\partial^2 P_0}{\partial L^2} - \frac{2(T-t)e^{kT}-\frac{2}{k}(e^{kT}-e^{kt})}{k}\frac{\partial P_0}{\partial L}\right) \\
&\quad +V_1(z)\left(\frac{\frac{e^{2kT}}{k}(e^{kT}-e^{kt})-\frac{1}{3k}(e^{3kT}-e^{3kt})}{k}\frac{\partial^3 P_0}{\partial L^3} - \frac{\frac{2e^{kT}}{k}(e^{kT}-e^{kt})-\frac{e^{2kT}-e^{2kt}}{k}}{k}\frac{\partial^2 P_0}{\partial L^2}\right) \\
&\quad -2(T-t)\frac{V_0(z)}{\overline{\sigma}(z)}u_h + \frac{2}{k}(e^{kT}-e^{kt})\frac{V_1(z)}{\overline{\sigma}(z)}\frac{\partial u_h}{\partial L}.
\end{aligned}
$$

Using (4.16), we eliminate u_h from the above expression and obtain:

$$
\begin{aligned}
&P_{0,1} \\
&= V_0(z)\Big[\frac{\frac{1}{2k}(e^{2kT}-e^{2kt})-(T-t)e^{2kT}}{k}\frac{\partial^2 P_0}{\partial L^2} - \frac{\frac{2}{k}(e^{kT}-e^{kt})-2(T-t)e^{kT}}{k}\frac{\partial P_0}{\partial L} \\
&\quad -\frac{2(T-t)}{\overline{\sigma}}\frac{\partial P_0}{\partial \overline{\sigma}} + \frac{(T-t)}{k}(e^{2kT}-e^{2kt})\frac{\partial^2 P_0}{\partial L^2} - \frac{2(T-t)}{k}(e^{kT}-e^{kt})\frac{\partial P_0}{\partial L}\Big] \\
&\quad +V_1(z)\Big[\frac{\frac{e^{2kT}}{k}(e^{kT}-e^{kt})-\frac{1}{3k}(e^{3kT}-e^{3kt})}{k}\frac{\partial^3 P_0}{\partial L^3} - \frac{\frac{2e^{kT}}{k}(e^{kT}-e^{kt})-\frac{e^{2kT}-e^{2kt}}{k}}{k}\frac{\partial^2 P_0}{\partial L^2} \\
&\quad +\frac{2(e^{kT}-e^{kt})}{k\overline{\sigma}}\frac{\partial^2 P_0}{\partial L\partial \overline{\sigma}} - \frac{(e^{kT}-e^{kt})(e^{2kT}-e^{2kt})}{k^2}\frac{\partial^3 P_0}{\partial L^3} + \frac{2(e^{kT}-e^{kt})^2}{k^2}\frac{\partial^2 P_0}{\partial L^2}\Big] \\
&= V_0(z)\Big[\frac{\frac{1}{2k}(e^{2kT}-e^{2kt})-(T-t)e^{2kt}}{k}\frac{\partial^2 P_0}{\partial L^2} - \frac{\frac{2}{k}(e^{kT}-e^{kt})-2(T-t)e^{kt}}{k}\frac{\partial P_0}{\partial L} \\
&\quad -\frac{2(T-t)}{\overline{\sigma}}\frac{\partial P_0}{\partial \overline{\sigma}}\Big] \\
&\quad +V_1(z)\Big[\frac{\frac{e^{2kt}}{k}(e^{kT}-e^{kt})-\frac{1}{3k}(e^{3kT}-e^{3kt})}{k}\frac{\partial^3 P_0}{\partial L^3} - \frac{\frac{2e^{kt}}{k}(e^{kT}-e^{kt})-\frac{e^{2kT}-e^{2kt}}{k}}{k}\frac{\partial^2 P_0}{\partial L^2} \\
&\quad +\frac{2(e^{kT}-e^{kt})}{k\overline{\sigma}}\frac{\partial^2 P_0}{\partial L\partial \overline{\sigma}}\Big]
\end{aligned}
\tag{4.18}
$$

Hence, the slow timescale asymptotic solution, $P_{0,1}$, is a linear combination of gamma, delta-gamma, vega, delta-vega, and a boundary correction term.

The first order approximation for P is now clear to be

$$\widetilde{P} = P_0 + \sqrt{\epsilon}P_{1,0} + \sqrt{\delta}P_{0,1}, \tag{4.19}$$

where P_0, $P_{1,0}$, and $P_{0,1}$ can be found in Theorem 4.2.1, (4.12), and (4.18), respectively.

To interpret the pricing formula, we inverse the transformation to have the price function in terms of F instead of L and we have the following proposition.

Proposition 4.2.1. The first order approximation $\widetilde{P}$ for P is

$$\widetilde{P} = P_0 + \sqrt{\epsilon}P_{1,0} + \sqrt{\delta}P_{0,1},$$

where,

$$
\begin{aligned}
& P_{1,0} \\
= \ & V_2(z)\Big(\frac{e^{2k(T-t)} - 2e^{k(T-t)} + 1}{2k}F\frac{\partial P_0}{\partial F} + \frac{e^{2k(T-t)} - 1}{2k}F^2\frac{\partial P_0}{\partial F}\Big) \\
& -V_3(z)\Big(\frac{2e^{3k(T-t)} - 3e^{2k(T-t)} + 1}{6k}F\frac{\partial P_0}{\partial F} + \frac{2e^{3k(T-t)} - e^{2k(T-t)} - 1}{2k}F^2\frac{\partial^2 P_0}{\partial F^2} \\
& +\frac{e^{3k(T-t)} - 1}{3k}F^3\frac{\partial^3 P_0}{\partial F^3}\Big),
\end{aligned}
$$

$$
\begin{aligned}
& P_{0,1} \\
= \ & V_0(z)\Big[\frac{\frac{e^{2k(T-t)}-1}{2k} + T - t - \frac{2(e^{k(T-t)}-1)}{k}}{k}F\frac{\partial P_0}{\partial F} + \frac{\frac{e^{2k(T-t)}-1}{2k} - (T-t)}{k}F^2\frac{\partial^2 P_0}{\partial F^2} \\
& -\frac{2(T-t)}{\overline{\sigma}}\frac{\partial P_0}{\partial \overline{\sigma}}\Big] \\
& +V_1(z)\Big[\frac{-\frac{e^{3k(T-t)}-1}{3k} + \frac{e^{2k(T-t)}-1}{k} + \frac{e^{k(T-t)}-1}{k}}{k}F\frac{\partial P_0}{\partial F} \\
& +\frac{-\frac{e^{3k(T-t)}-1}{k} + \frac{e^{2k(T-t)}-1}{k} + \frac{e^{k(T-t)}-1}{k}}{k}F^2\frac{\partial^2 P_0}{\partial F^2}
\end{aligned}
$$

$$+ \frac{-\frac{e^{3k(T-t)}-1}{3k} + \frac{e^{k(T-t)}-1}{k}}{k} F^3 \frac{\partial^3 P_0}{\partial F^3} + \frac{2(e^{k(T-t)}-1)}{k\bar{\sigma}} F \frac{\partial^2 P_0}{\partial F \partial \bar{\sigma}}]$$

and P_0 is shown in (4.10).

4.3 Simulation studies

We simulate the asset price process using a fully specified SV model under risk-neutral measure:

$$
\begin{aligned}
dF_t &= [k(\log \bar{F} - \log F_t) + r - r_f] F_t dt + e^{Y_t + Z_t} F_t dW_t^{(0)*}, \\
dY_t &= \left[\frac{1}{\epsilon}(m_1 - Y_t) - \frac{\nu_1\sqrt{2}}{\sqrt{\epsilon}}\Lambda \right] dt + \frac{\nu_1\sqrt{2}}{\sqrt{\epsilon}} dW_t^{(1)*}, \\
dZ_t &= \left[\delta(m_2 - Z_t) - \sqrt{\delta}\nu_2\Gamma \right] dt + \sqrt{\delta}\nu_2 dW_t^{(2)*}.
\end{aligned}
\tag{4.20}
$$

Here we assume $f(Y, Z) = e^{Y+Z}$, $c(Z_t) = (m_2 - Z_t)$ and $g(Z_t) = \nu_2$ in (4.1) in our simulation. All other parameters are constants. We use a time-space of $1/250$ to generate 80,000 sample paths with the Euler method.

Given that $f(y, z) = e^{y+z}$, it is easy to express effective parameters V_0, V_1, V_2, V_3, and $\bar{\sigma}$ in terms of the original set of model parameters. Specifically,

$$
\begin{aligned}
V_0 &= \frac{1}{2}\nu_2\Gamma e^{2(z+m_1+\nu_1^2)}, \quad V_1 = \frac{1}{2}\nu_2\rho_2 e^{3z+3m_1+\frac{5}{2}\nu_1^2}, \\
V_2 &= \frac{\Lambda}{\nu_1\sqrt{2}} \left[m_1 e^{2(z+m_1+\nu_1^2)} - (m_1 + \nu_1^2)e^{2z+m_1+\frac{1}{2}\nu_1^2} \right], \\
V_3 &= \frac{\rho_1}{\nu_1\sqrt{2}} \left[e^{3z+3m_1+\frac{5}{2}\nu_1^2} - e^{3z+3m_1+\frac{9}{2}\nu_1^2} \right], \quad \bar{\sigma} = e^{z+m_1+\nu_1^2}.
\end{aligned}
\tag{4.21}
$$

The regularity condition for $f(x, y)$ is violated with this choice of volatility function and we put ourselves in a theoretically weaker condition. Our approximation

is expected to performs better for a regulated volatility function. Even in this case, our simulation shows that this choice still offers a high quality of estimation of option prices. Setting the volatility function to an exponential function is solely for computational convenience.

We evaluate the accuracy of the price approximation for the European call option. We allow δ and ϵ to change but fix the parameters: $k = 0.05\%, r = 5\%, r_f = 0\%, \Lambda = 0, \Gamma = -0.2, m_1 = -0.8, m_2 = -1.8, \nu_1 = 0.5, \nu_2 = 1.13, \rho_1 = \rho_2 = -0.2, \rho_{12} = 0, Y_0 = -1, Z_0 = -1, F_0 = \bar{F} = 100$ and $T = 3$. Most parameters are used in Fouque and Han (2004).

In Table 4.1, we present the simulation results with setting δ to zero and varying the ϵ. This consideration corresponds to the one-factor SV model of Fouque et al. (2000) that the mean-reverting rate, $1/\epsilon$, of the volatility is assumed to be fast.

As the fast mean-reverting SV model is nested in our framework by setting δ to zero, we also examine the accuracy of our price approximation for this model. Monte Carlo simulation is regarded as the benchmark to compute the percentage error. Although both Black-Scholes price and asymptotic prices deviate from the benchmark option price, we see from Table 4.1 that the errors generated by the asymptotic approximation are smaller. Comparing with the Black-Scholes price, our approximation has an obvious improvement on pricing. We can also observe that the pricing error is decreasing with the value of ϵ and δ which supports the convergence of the model. On the other hand, the asymptotic approximation is

much more efficient than the Monte Carlo simulation. In fact, the Monte Carlo simulation takes more than 20 minutes to obtain an option price, whereas the asymptotic formula takes less than 1 second.

Strike Price (K)	Monte Carlo simulation	Black-Scholes price (error)	Asymptotic price (error)
$\epsilon = 0.02, \delta = 0.00$			
80	31.7901	31.7653(0.08%)	31.7864 (0.01%)
90	25.5098	25.2466(1.03%)	25.2707 (0.08%)
100	19.7487	19.6882(0.31%)	19.7155 (0.17%)
$\epsilon = 0.1, \delta = 0.00$			
80	31.5903	31.8125 (0.70%)	31.7653(0.55%)
90	25.1987	25.3006 (0.40%)	25.2466(0.19%)
100	19.5603	19.7492 (0.97%)	19.6882(0.65%)

Table 4.1: Fast mean-reverting SV

We report the accuracy of the price approximation with the two-factor SV model in Table 4.2 where we carry out simulations with different combinations of δ and ϵ. As our asymptotic solution involves two approximation steps on the processes of Y and Z respectively, its accuracy is expected not to be as good as the fast mean-reverting case. Fortunately, it turns out that the asymptotic approximation still provides a high quality of estimation of option price. Once

Strike Price (K)	Monte Carlo simulation	Black-Scholes price (error)	Asymptotic price (error)
$\epsilon = 0.02, \delta = 0.02$			
80	32.4396	31.7653(2.08%)	32.2932(0.45%)
90	25.8177	25.2466(2.21%)	25.8729(0.21%)
100	20.3592	19.6882(3.30%)	20.4181(0.29%)
$\epsilon = 0.1, \delta = 0.1$			
80	32.4987	31.7653(2.26%)	32.9457(1.38%)
90	26.2629	25.2466(3.87%)	26.6470(1.46%)
100	20.5634	19.6882(4.26%)	21.3202(3.68%)

Table 4.2: Multiscale mean-reverting SV

again, we regard the Monte Carlo simulation as the benchmark to compute the percentage error.

From Table 4.2, we see that the pricing errors are no greater than 0.5% when the δ is set to 0.02. Empirical studies report that δ is of this order of magnitude. The BS price generates an absolute pricing error over 2% even for a small value of δ. In case the δ is getting larger to reach the value of 0.1, the percentage error of the asymptotic formula is getting poor, whereas the BS price is getting more terribly poor. Therefore, the asymptotic formula consistently outperforms the BS price.

All in all, we learn that the asymptotic formula outperforms the BS approach under both fast mean-reverting SV and multiscale volatility models when underlying asset follows the mean-reverting lognormal process. The asymptotic approach is less accurate, but still improves the BS formula, if either ϵ or δ is larger than 0.1.

Chapter 5

Conclusion

This thesis has proposed a new asset price dynamics to accommodate both mean reversion and stochastic volatility for many financial assets. The proposed model with mean-reverting underlying process and stochastic volatility following Heston Model has been applied to pricing European options and exotic options. Specifically, analytical solutions are derived for the characteristic function and the European options. The proposed model can fit the observed future prices of the underlying assets and the volatility smile within a unified framework. A trinomial tree lattice approach was developed to value barrier and American options. Numerical examples show that the lattice approach is accurate and efficient. Furthermore, Multiscale stochastic volatility model is also investigated. The underlying asset price is assumed to follow mean-reverting lognormal process with a stochastic volatility driven by two stochastic processes with one persistent factor and one fast mean-reverting factor. Semi-analytical pricing formulas for

European option is derived by means of multiscale asymptotic techniques. Numerical examples show that the price approximation is accurate.

Appendix

A   Verifications

A.1   Proof of Lemma 3.1.1

Feynman-Kac formula gives the following PDE for the characteristic function.

$$\frac{v}{2}f_{xx} + \rho\sigma v f_{xv} + \frac{\sigma^2 v}{2}f_{vv} + (\theta(t) - \kappa x - \frac{v}{2})f_x + (a(t) - bv)f_v + f_t = 0,$$

$$f(x, v, T; \phi) = e^{i\phi x}. \tag{1}$$

To see this, we apply Ito Lemma to $\{f(x, v, s; \phi)\}_{t \leq s \leq T}$, and obtain

$$f(x_T, v_T, T; \phi)$$

$$= f(x_t, v_t, t; \phi) + \int_t^T \sqrt{v}f_x dW_s^{(0)} + \int_t^T \sigma\sqrt{v}f_v dW_s^{(1)}$$

$$+ \int_t^T \left(\frac{v}{2}f_{xx} + \rho\sigma v f_{xv} + \frac{\sigma^2 v}{2}f_{vv} + (\theta(t) - \kappa x - \frac{v}{2})f_x + (a(t) - bv)f_v + f_t\right) ds$$

Taking expectation both sides and recognizing the fact that $f(x_T, v_T, T; \phi) = e^{i\phi x_T}$ would then give the result. Consider an exponential affine form for the characterisitic function:

$$f(x, v, t; \phi) = \exp\left(B(\tau) + C(\tau)x + D(\tau)v + i\phi x\right),$$

61

where $\tau = T - t$ and $B(\tau = 0) = C(\tau = 0) = D(\tau = 0) = 0$. Subsituting it into (1) yields

$$0 = v[\frac{1}{2}(C(\tau) + i\phi)^2 + \rho\sigma D(\tau)(C(\tau) + i\phi) + \frac{1}{2}\sigma^2 D^2(\tau)$$

$$-\frac{1}{2}(C(\tau) + i\phi - bD(\tau)) - D'] + x[-\kappa(C(\tau) + i\phi) - C'] +$$

$$[\theta(T - \tau)(C(\tau) + i\phi) + a(t)D(\tau) - B'],$$

where the differentiations are taken with respect to τ. This leads to the following system of ODEs:

$$0 = \frac{1}{2}(C(\tau) + i\phi)^2 + \rho\sigma D(\tau)(C(\tau) + i\phi)$$

$$+\frac{1}{2}\sigma^2 D^2(\tau) - \frac{1}{2}(C(\tau) + i\phi) - bD(\tau) - D', \qquad (2)$$

$$0 = -\kappa(C(\tau) + i\phi) - C', \qquad (3)$$

$$0 = \theta(t)(C(\tau) + i\phi) + aD(\tau) - B'. \qquad (4)$$

It is clear from (3) and $C(0) = 0$ that

$$C(\tau) = i\phi e^{-\kappa\tau} - i\phi. \qquad (5)$$

Subsituting (5) into (2), we have

$$-D' = -\frac{1}{2}\sigma^2 D^2 + (b - \rho\sigma i\phi e^{-\kappa\tau})D + \frac{1}{2}(i\phi e^{-\kappa\tau} + \phi^2 e^{-2\kappa\tau}). \qquad (6)$$

Using the transformation of independent variable $y = e^{-\kappa\tau}$ and defining $\tilde{D}(y) = D(\tau)$, (6) becomes a Ricatti equation

$$\frac{d\tilde{D}}{dy} = -\frac{1}{2\kappa y}\sigma^2 \tilde{D}^2 + (\frac{b}{\kappa y} - \frac{\rho\sigma i\phi}{\kappa})\tilde{D} + \frac{1}{2\kappa}(i\phi + \phi^2 y), \quad \tilde{D}(1) = 0. \qquad (7)$$

To solve (7), we need a particular solution from which the general solution can be derived for the Ricatti equation. Consider the transformation:

$$\widetilde{D}(y) = \frac{2\kappa y w'(y)}{\sigma^2 w(y)}. \tag{8}$$

Hence,

$$y w''(y) - [(\frac{b}{\kappa} - 1) - y(\frac{\rho\sigma i\phi}{\kappa})]w'(y) - (\frac{i\phi\sigma^2}{4\kappa^2} + \frac{\sigma^2\phi^2}{4\kappa^2}y)w(y) = 0. \tag{9}$$

The ODE (9) has a general solution of the form, see Zwillinger (1992),

$$w(y) = e^{(\sqrt{(1-\rho^2)}-\rho i)\frac{\sigma\phi}{2\kappa}y}[C_1\Phi(a^*, b^*, \frac{y}{\lambda}) + C_2 y^{1-b^*}\Phi(a^* - b^* + 1, 2 - b^*, \frac{x}{\lambda})] \tag{10}$$

where a^*, b^* and λ are defined in the Lemma, C_1 and C_2 are two constants to be determined from boundary conditions, and $\Phi(a, b, z)$ is the degenerated hypergeometric function which has Kummer's series expression:

$$\Phi(a, b, z) = 1 + \sum_{k=1}^{\infty} \frac{(a)_k z^k}{(b)_k k!}, (a)_k = a(a+1)...(a+k-1).$$

By letting $C_1 = 1$ and $C_2 = 0$ in (10), we obtain a particular solution for (9) as

$$w(y) = e^{(\sqrt{(1-\rho^2)}-\rho i)\frac{\sigma\phi}{2\kappa}y}\left[\Phi(a^*, b^*, \frac{y}{\lambda})\right].$$

Using (8), a particular solution for (7) is obtained as $U(y)$ which is defined in the Lemma. Therefore, the general solution for (7) is, see Zwillinger (1992),

$$\begin{aligned}
\widetilde{D}(y) &= U(y) + \frac{e^{\int_1^y \frac{-\sigma^2}{\kappa x}U(x)+\frac{b}{\kappa x}-\frac{\rho\sigma i\phi}{\kappa}dx}}{-\frac{1}{U(1)} - \int_1^y (\frac{-\sigma^2}{2\kappa\xi})(e^{\int_1^\xi \frac{-\sigma^2}{\kappa x}U(x)+\frac{b}{\kappa x}-\frac{\rho\sigma i\phi}{\kappa}dx})d\xi} \\
&= U(y) + \frac{\frac{\Phi^2(a^*,b^*,\frac{1}{\lambda})}{\Phi^2(a^*,b^*,\frac{y}{\lambda})}y^{\frac{b}{\kappa}}e^{-2(\sqrt{1-\rho^2})\frac{\sigma\phi}{2\kappa}(y-1)}}{-\frac{1}{U(1)} + \frac{\sigma^2}{2\kappa}\int_1^y \frac{\Phi^2(a^*,b^*,\frac{1}{\lambda})}{\Phi^2(a^*,b^*,\frac{\xi}{\lambda})}\xi^{\frac{b}{\kappa}-1}e^{-2(\sqrt{1-\rho^2})\frac{\sigma\phi}{2\kappa}(\xi-1)}d\xi}.
\end{aligned}$$

63

From (4), we obtain

$$
\begin{aligned}
B(\tau) &= \int_0^\tau \theta(t)(C(\tau)+i\phi)+a(t)D(\tau)d\tau \\
&= \int_{T-\tau}^T \theta(t)i\phi e^{-\kappa(T-t)}dt + \int_{T-\tau}^T a(t)D(T-t)dt.
\end{aligned}
$$

B   Black-Scholes Greeks

Black-Scholes Formula for call Option with mean reversion underlying process

$$
P_0 = \hat{L}e^{-r(T-t)}N(d_1) - Ke^{-r(T-t)}N(d_2),
$$

where

$$
\begin{aligned}
\hat{L} &= e^{L_t e^{-kT} + \frac{(\theta - \frac{\overline{\sigma}(z)^2}{2})}{k}(1-e^{-k(T-t)}) + \frac{v^2}{2}} = F_t e^{-k(T-t)} e^{\frac{(\theta - \frac{\overline{\sigma}(z)^2}{2})}{k}(1-e^{-k(T-t)}) + \frac{v^2}{2}}, \\
v^2 &= \frac{\overline{\sigma}(z)^2 e^{-2k(T-t)}}{2k}(e^{2k(T-t)} - 1), \\
d_1 &= \frac{\ln(\frac{\hat{L}}{K}) + \frac{v^2}{2}}{v}, \quad d_2 = d_1 - v,
\end{aligned}
$$

Greeks for the Call Option with mean reversion underlying process

$$\frac{\partial P_0}{\partial L_t} = e^{-kT}e^{-r(T-t)}N(d_1)\hat{L}$$

$$\frac{\partial^2 P_0}{\partial L_t^2} = e^{-2kT}e^{-r(T-t)}\left(N'(d_1)\frac{\hat{L}}{v} + N(d_1)\hat{L}\right)$$

$$\frac{\partial^3 P_0}{\partial L_t^3} = e^{-3kT}e^{-r(T-t)}\left(N''(d_1)\frac{\hat{L}}{v^2} + 2N'(d_1)\frac{\hat{L}}{v} + N(d_1)\hat{L}\right)$$

$$N'(d_1) = \frac{\partial N(d_1)}{\partial d_1} = \frac{1}{\sqrt{2\pi}}e^{-\frac{d_1}{2}}$$

$$N''(d_1) = \frac{\partial^2 N(d_1)}{\partial d_1^2} = -\frac{1}{2\sqrt{2\pi}}e^{-\frac{d_1}{2}}$$

$$\frac{\partial P_0}{\partial \overline{\sigma}} = \hat{L}e^{-r(T-t)}N'(d_1)\sqrt{\frac{1-e^{-2k(T-t)}}{2k}}$$
$$+2e^{-r(T-t)}N(d_1)\overline{\sigma}\hat{L}\left(\frac{1-e^{-2k(T-t)}}{4k} - \frac{1-e^{-k(T-t)}}{2k}\right)$$

$$\frac{\partial^2 P_0}{\partial L_t \partial \overline{\sigma}} = \hat{L}e^{-r(T-t)-kT}\sqrt{\frac{1-e^{-2k(T-t)}}{2k}}\left(N'(d_1) + \frac{N''(d_1)}{v}\right)$$
$$+2\hat{L}e^{-r(T-t)-kT}\overline{\sigma}\left(\frac{1-e^{-2k(T-t)}}{4k} - \frac{1-e^{-k(T-t)}}{2k}\right)\left(N(d_1) + \frac{N'(d_1)}{v}\right)$$

Bibliography

[1] Alaton, P., Djehiche, B. and Stillberger, D. (2002). On Modelling and Pricing Weather Derivatives. Applied Mathematical Finance, 9(1), 1–20.

[2] Bakshi, G., Cao, C., Chen, Z. (1997). Empirical Performance of Alternative Option Pricing Models. Journal of Finance, 52, 2003–43.

[3] Benth, F. E. and Saltyte-Benth, J. (2007). The Volatility of Temperature and Pricing of Weather Derivatives. Quantitative Finance, 7, 553–561.

[4] Bessembinder, H., Coughenour, J.F., Seguin, P.J. and Smoller, M.M. (1995). Mean Reversion in Equilibrium Asset Prices: Evidence from the Futures Term Structure. Journal of Finance, 50, 361–375.

[5] Cadenillas, A., Sarkar, S., Zapatero, F. (2007). Optimal Dividend Policy with Mean-Reverting Cash Reservoir. Mathematical Finance, 17, 81–109.

[6] Carr, P. and Madan, D. (1999) Option Pricing and the Fast Fourier Transform Journal of Computational Finance, 2, 61–73.

[7] Cecchetti, S.G., Lam, P-S. and Mark, N.C. (1990). Mean Reversion in Equilibrium Asset Prices. American Economic Review, 80, 398–418.

[8] Chan, N.H. and Wong, H.Y. (2006). Simulation Techniques in Financial Risk Management, Wiley, New York. Book Review of JASA (2007) pp758-759.

[9] Davydov, D., and Linetsky, V. (2001). Pricing and Hedging Path Dependent Options under the CEV Process. Management Science, 47, 949-965.

[10] Deng, S. J. (1999). Stochastic Models of Energy Commodity Prices and Their Applications: Mean-Reversion with Jumps and Spikes. POWER working paper, University of California Energy Institute, Berkeley.

[11] Dornier, F. and Querel, M. (2000). Caution to the Wind. Energy Power Risk Management, Weather Risk Special Report, August, 30-32.

[12] Ekvall, N., Jennergren, L. P., and Naslund, B. (1997). Currency Option Pricing with Mean Reversion And Uncovered Interest Parity: A Revision of the Garman-Kohlhagen Model. European Journal of Operational Research, 100, 41–59.

[13] Fouque, J.P., G. Papanicolaou, and R. Sircar, *Derivatives in Financial Markets with Stochastic Volatility*, Cambridge: Cambridge University Press, 2000.

[14] Fouque, J.P., G. Papanicolaou, and R. Sircar, K. Solna, Singular Perturbations in Option Pricing, *SIAM Journal on Applied Mathematics* 63(5), 1648-1665, 2003a.

[15] Fouque, J.P., G. Papanicolaou, R. Sircar, and K. Solna, Multiscale Stochastic Volatility Asymptotics, *SIAM Journal on Multiscale Modeling and Simulation* 2(1), 22-42, 2003b.

[16] Fouque, J.P., C.H. Han, Pricing Asian Options with Stochastic Volatility, *Quantitative Finance* 3, 353-362, 2003.

[17] Heston, S. (1993). A Closed-Form Solution of Options with Stochastic Volatility with Applications to Bond and Currency Options. The Review of Financial Studies, 6, 327–343.

[18] Hilliard, J.E., and Schwartz, A. (1996). Binomial Option Pricing under Stochastic Volatility And Correlated State Variables. Journal of Derivatives, 23–39, Fall.

[19] Hull, J. and White, A. (1993). One-Factor Interest-Rate Models and the Valuation of Interest-Rate Derivative Securities. Journal of Financial and Quantitative Analysis, 28(2), 235–254.

[20] Hui, C.H. and Lo, C.F. (2006). Currency Barrier Option Pricing with Mean Reversion. The Journal of Futures Markets, 26, 939–958.

[21] Poterba, J. and Summers, L. (1988). Mean Reversion in Stock Prices: Evidence and Implications. Journal of Financial Economics 22, 27–59.

[22] Sorensen, C. (1997). An Equilibrium Approach to Pricing Foreign Currency Options. European Financial Management, 3, 63–84.

[23] Jorion, P., and Sweeney, R.J. (1996). Mean Reversion in Real Exchange Rates: Evidence and Implications for Forecasting. Journal of International Money and Finance, 15, 535–550.

[24] Lewis, A.L. (2001). A Simple Option Formula for General Jump-Diffusion and Other Exponential Lévy Processes. The 8th Annual CAP Workshop on Derivative Securities and Risk Management, November.

[25] Schwartz, E. S. (1997). The Stochastic Nature of Commodity Prices: Implications for Valuation and Hedging. Journal of Finance, 52, 923–73.

[26] Sweeney, R.J. (2006). Mean Reversion in G-10 Nominal Exchange Rates. Journal of Financial and Quantitative Analysis, 41, 685–708.

[27] Wong, H.Y. and Chan, C.M. (2007). Lookback Options and Dynamic fund Protection under Multiscale Stochastic Volatility, Insurance: Mathematics and Economics, 40(3) 357-385, 2007.

[28] Wong, H.Y. and Chan, C.M. (2008). Turbo Warrants under Stochastic Volatility. To appear in Quantitative Finance.

[29] Wong, H.Y. and Cheung, Y.L. (2004). Geometric Asian Options: Valuation and Calibration With Stochastic Volatility, *Quantitative Finance* 4, 301-314.

[30] Wong, H.Y. and Lau, K.Y. (2008). Path-Dependent Currency Options with Mean Reversion. The Journal of Futures Markets, 28, 275–293.

[31] Wong, H.Y. and Lo, Y.W. (2008). Option Pricing with Mean Reversion and Stochastic Volatility. To appear in European Journal of Operational Research.

[32] Zwillinger, D. (1992). Handbook of Differential Equations. Boston: Academic Press.